POLITECNICO DI TORINO

Master degree course in Biomedical Engineering

Master Degree Thesis

MEMS Microphones for Muscle Fatigue Monitoring: a Tool for Spinal Cord Injury Rehabilitation

Supervisors:
Prof. Danilo Demarchi
Prof. Sandro Carrara
Dr. Paolo Motto Ros

Candidate
Sofia Milanese
matricola: 231489

July 2018

To my family,
with pride,
gratitude
and infinite love.

Sommario

Le lesioni al midollo spinale richiedono tecniche riabilitative e assistenza multidisciplinari ed efficaci, al fine di migliorare significativamente la qualità della vita dei pazienti. Un danno al midollo spinale provoca conseguenze importanti sulle funzionalità del soggetto leso, portando ad una disabilità rilevante. Quando il percorso del segnale nervoso proveniente dal cervello viene interrotto a causa di una lesione al midollo, il paziente non è più in grado di compiere contrazioni volontarie dei muscoli nell'area colpita, mancando anche di feedback sensoriali quali il tatto o la fatica muscolare nel caso la disabilità sia completa. La riabilitazione dei soggetti con lesioni al midollo spinale ha inizialmente lo scopo di prevenire i danni collaterali dell'immobilità, per poi concentrarsi sull'indipendenza del paziente nelle attivitá quotidiane principali. Gli esercizi proposti spesso richiedono l'utilizzo di stimolatori elettrici, capaci di indurre una contrazione muscolare bypassando il sistema nervoso centrale. La stimolazione elettrica non invasiva induce maggiore fatica nel muscolo rispetto alla contrazione volontaria, rappresentando un ostacolo durante gli esercizi di riabilitazione. I sistemi riabilitativi basati su stimolazione elettrica funzionale presentano quindi una migliore stabilità ed efficacia se dotati di un feedback di fatica muscolare. Nel corso del primo capitolo si tratterà della riabilitazione al midollo spinale, con particolare attenzione sugli aspetti relativi alla fatica muscolare durante stimolazione elettrica.

La fatica muscolare viene studiata analizzando diversi tipi di segnali biomedici. In particolare, la meccanomiografia si è rivelata uno strumento utile all'analisi della fatica muscolare, presentando diversi vantaggi rispetto alle tecniche tradizionali. Il segnale meccanomiografico (MMG) rappresenta l'attività meccanica del muscolo, che si esprime come una vibrazione a bassa frequenza (2-120 Hz) della superficie della pelle. Durante una stimolazione elettrica, l'acquisizione del segnale meccanomiografico non viene influenzata da artefatti di stimolazione, in quanto la natura del segnale è di tipo meccanico. Inoltre, il posizionamento del trasduttore sul muscolo di interesse non influenza in modo significativo il segnale risultante quanto nel caso del segnale elettromiografico. L'esposizione dei diversi metodi per la valutazione della fatica muscolare, in particolare tramite meccanomiogramma acquisito con microfoni

capacitivi, verrà sviluppata nel secondo capitolo.

Lo scopo di questo lavoro di tesi è quello di progettare un sistema per il monitoraggio dell'affaticamento del paziente nel trattamento riabilitativo, specialmente quello in cui viene adottato la stimolazione elettrica di pazienti con lesioni al midollo spinale in modo da fornire un feedback al terapista. Per la realizzazione di tale sistema, due diversi tipi di microfoni sono stati considerati e confrontati: (i) microfono capacitivo MEMS *ST Microelectronics* e (ii) microfono MEMS capacitivo analogico *Knowles*. Due camere acustiche coniche identiche sono state progettate e integrate nei loro *case*, tramite l'utilizzo della tecnologia di stampa 3D. L'acquisizione del microfono digitale viene gestita da un'applicazione per smartphone resa disponibile da *ST Microelectronics*, mentre il microfono analogico viene gestito dalla scheda *BITalino Plugged Board* prodotta da *Plux wireless biosignals*. La scheda riceve i parametri di acquisizione e invia i dati del microfono tramite tecnologia Bluetooth, al fine di migliorare l'indossabilità del sistema. Il terzo capitolo descriverà le diverse parti del sistema, con la completa strumentazione hardware e software.

La validazione del sistema di feedback di fatica muscolare è stata effettuata su soggetti sani, durante contrazioni isometriche del bicipite. I segnali acquisiti sono: (i) segnale elettromiografico tramite elettrodi di superficie, (ii) segnale meccanomiografico tramite microfono MEMS capacitivo digitale e (iii) segnale meccanomiografico tramite microfono MEMS capacitivo analogico. Il primo è stato considerato come segnale standard per la valutazione della fatica muscolare. Il microfono analogico è stato introdotto perchè precedentemente validato in letteratura per questa applicazione, in modo da rappresentare un riferimento per la valutazione del comportamento del microfono digitale. Da ogni segnale sono stati estratti parametri di ampiezza e frequenza al fine di osservare i loro trend durante l'evoluzione della contrazione. Entrambi i microfoni hanno dimostrato di essere adatti per l'acquisizione del segnale MMG, mostrando i trend corretti per i parametri di fatica. I trend ottenuti da i due diversi microfoni hanno mostrato una correlazione consistente sottolineando l'idoneità del microfono digitale per questo tipo di applicazione. In particolare, la correlazione tra i parametri di ampiezza è risultata essere maggiore di 0.9. Osservando i risultati statistici tra i soggetti, il segnale dei trasduttori acustici ha presentato una minore variabilità rispetto al segnale elettromiografico, dimostrando una maggiore robustezza rispetto allo standard. Nel quarto capitolo verrà descritta la modalità di validazione del sistema e i risultati ottenuti, la cui analisi e discussione verranno esposti nel quinto capitolo. Il sesto capitolo ricapitolerá i principali raggiungimenti della tesi e proporrà possibili future applicazioni per concludere la trattazione.

Summary

Spinal cord injuries (SCI) require multisciplinary rehabilitation and assistive techniques, in order to substantially improve the patients' quality of life. Whatever damage at the spinal cord causes a significant impairment to the subject's functionalities and a relevant disability. In the case of a disrupt communication caused by a spinal cord injury, the patient is no more able to perform voluntary contractions of the muscles involved, lacking a sensory feedback, such as touch or muscle fatigue in case of complete damage. Rehabilitation of injured patients aims at first to prevent immobility collateral damages, then the focus moves to the subject independency during daily tasks. The proposed exercises often involve electrical stimulators, able to induce a muscular contraction bypassing the central nervous system. Non-invasive electrical stimulation induces higher muscular fatigue with respect to a voluntary contraction. This represents an obstacle during rehabilitation tasks. Functional electrical stimulation systems present a better stability and reliability if provided with a muscle fatigue feedback. During the first chapter the spinal cord injury rehabilitation will be illustrated, in particular focusing on muscle fatigue during electrical stimulation.

Muscle fatigue is assessed by the analysis of various biomedical signals. In particular, mechanomyography (MMG) proved to be a suitable tool for muscle fatigue analysis. This signal presents some benefits with respect to traditional techniques. Mechanomyography represents the mechanical activity of the muscle, expressed as a low frequency (2-120 Hz) vibration on the skin surface. During an electrical stimulation, the mechanomyography acquisition is not affected by stimulation artifacts, due to the mechanical origin of the signal. Moreover, the transducer placement does not significantly influence the resulting signal with respect to the electromyographic signal recording. The second chapter will concern the exposition of the different muscle fatigue assessment techniques, in particular by means of condenser microphones for mechanomyography recording.

The purpose of this thesis project is to design an effective muscle feedback system, in particular in order to make it suitable for rehabilitation of SCI patients by means

of electrical stimulation. Therefore *Micro Electro-Mechanical System* (MEMS) technology condenser microphones were considered, because of their small dimensions and high integrability. In particular, two different microphones were selected: (i) *ST Microelectronics* MEMS condenser digital microphone and (ii) *Knowles* MEMS condenser analog microphone. Two identical, conical acoustic chambers were designed and integrated on their plastic cases, exploiting 3D printing techniques. The digital microphone acquisition is managed by a *ST Microelectronics* smartphone application. The analog microphone on the other hand is managed by the *BITalino Plugged Board* by *Plux wireless biosignals.* The board is programmed to receive recording parameters and to send microphone data by means of Bluetooth technology, to improve the system wearability. The third chapter will describe in details the complete hardware and software instrumentation.

The muscle fatigue feedback system validation was carried out on healthy subjects, during isometric contractions of the biceps muscle. The acquired signal were: (i) electromyographic signal by means of surface electrodes, (ii) mechanomyographic signal by means of the digital MEMS condenser microphone and (iii) mechanomyographic signal by means of the analog MEMS condenser microphone. The first was considered as the standard signal for muscle fatigue evaluation. The analog microphone was introduced because previously validated in literature for this application, representing a reference for the assessment of the digital microphone suitability. Both amplitude and frequency parameters were extracted from each signal, in order to observe their trend during the contraction evolution. Both microphones demostrated their suitability for the mechanomyography signal acquisition, showing the correct fatigue parameters trends. The resulting trends from the two different microphones showed a relevant correlation, proving the digital transducer suitability for this application. In particular, the correlation coefficient between amplitude parameters is higher than 0.9. Considering the statistics results, the acoustic trasducers signal presents a lower variability with respect to the electromyographic signal. This highlights the consistent robustness of the mechanomyography fatigue assessment system when compared to the standard. In chapter 4 the validation protocols and obtained results will be exposed. The system discussion will take place in chapter 5, while the sixth chapter will debate its possible future applications.

Acknowledgements

I would like to express my gratitude to Professor Demarchi and Professor Carrara, for the opportunity to work at this project and for your guidance. My sincere thanks also go to Paolo Motto Ros and Francesca Stradolini, for the fundamental support you provide me throughout the whole work, and to Professor Carullo and Alessandro Sanginario for your helpful advice and support.

Contents

List of Figures

Acronyms

PCM *Pulse Code Modulation* 14

NIRS *Near Infra-Red Spectroscopy* 14

ODE *Open Development Environment* 17

DENERG *Dipartimento di Energia* 17

RSS *Reference Sound Source* 17

SLM *Sound Level Meter* 17

PDMS *Polydimethylsiloxane* 17

PCB *Printed Circuit Board* 20

ACI *Atelier de Fabrication de Circuits Imprimés* 20

EPFL *École Polytechnique Fédérale de Lausanne* 20

AFA *Atelier de Fabrication Additive* 21

ABS *Acrylonitrile Butadiene Styrene* 22

IDE *Integrated Development Environment* 22

GUI *Graphical User Interface* 22

ARV *Average Rectified Value* 24

RMS *Root Mean Square* 24

MF *Mean Frequency* 24

PSD *Power Spectral Density* 24

SENIAM *Surface ElectroMyoGraphy for the Non-Invasive Assessment of Muscles* 30

Chapter 1

Introduction

There are 2500 new *Spinal Cord Injury* (SCI) patients each year in Italy, considering that the 80% are in the 10-40 years age group. Multidisciplinary rehabilitation and assistive technologies are crucial for a better quality of life, especially considering the long life expectancy of the majority of these patients [15, 16]. In the following sections, the SCI condition and the most widely used rehabilitation techniques are explicated. In particular, the importance of muscle fatigue monitoring during *Functional Electrical Stimulation* (FES) training exercises is highlighted.

1.1 Spinal Cord Injury

The spinal cord is part of the human central nervous system, along with the enchephalon, and it is hosted and protected inside the vertebral column. The extension of the spinal cord begins at the brain stem and it ends in the lower back area at the *conus medularis*. The two main functions are: (i) to innervate the body muscles, by means of spinal nerves pairs generated at each division between adjacent vertebrae, and (ii) to receive sensory information through specific nerves. The spinal cord can be divided into 31 sections, corresponding to 5 main areas: cervical, thoracic, lumbar, sacral and coccygeal. At the cervical and lumbar level, the spinal cord is known to present larger dimensions, since the nerves emerging at these points innervate the limbs. In order to identify a specific vertebra of one of the aforesaid areas, a letter and a number are assigned to it. For example, T-1 is the first thoracic vertebra, while L-1 is the first lumbar vertebra [16, 17]. The conventional enumeration for the spinal cord vertebra has been reported in figure 1.1, as well as the description of the main motor and sensory functions at the different levels.

Any damage reported at whichever of these spinal cord areas leads to serious impairment of the subject. SCI is a disabling condition involving an interruption of communication between the central nervous system and the innervated body parts.

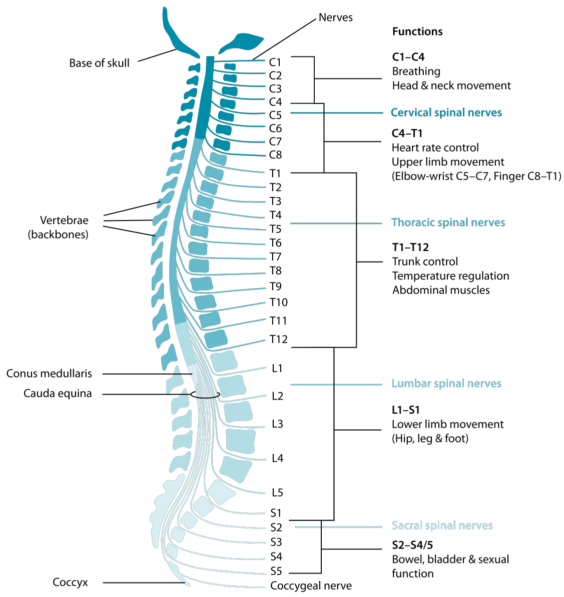

Figure 1.1: **Representation of the human spinal cord with the segments main functions.** Reprinted from [1].

The damage can be caused by a traumatic event, such as falls, car accidents or sports-related injuries, or non-traumatic events, for example due to some conditions like osteoarthritis, tumors and spina bifida [16, 1]. As spinal nerves are damaged, the motor and sensory functions of the involved body parts are compromised; if the injury is complete, a total loss of these functions is observed below the level of injury, while incompleteness preserves part of sensory and/or motor functions [16, 18]. The level of the damaged vertebra can be identified by X-rays analysis. On the other side, the neurological impairment is normally assessed by performing sensitivity tests on the patient's skin. The test is accomplished by dividing the patient's skin into separated areas, known as *dermatomes*; each dermatome corresponds to a different innervation level of the spinal cord. By stimulating each dermatome with pinpricks, it is possible to indicate the level of spinal cord injury depending on the sensory feedback provided by the subject. The patient's condition can be defined *tetraplegia* when all four limbs are submitted to impairment, or *paraplegia* when the level of injury only involves the lower part of the body.

1.2 Spinal Cord Injury Rehabilitation

SCI rehabilitation is crucial already from the early, acute stages of the disabling condition. During the first period of intervention (6-12 weeks), high care has to be taken in positioning the patient's joints with the help of supports (e.g. pillows or othosis) in order to maintain the articulary structure preventing from further complications. At first, rehabilitation is aimed to prevent immobility drawbacks, such as muscle atrophy and contractures, by frequently effecting passive exercises. During this rehabilitative phase, the *Range Of Motion* (ROM) exercises are proven to be effective. To accomplish these exercises, an occupational therapist moves the patient's limbs and joints reaching their full range of motion. In case the patient also presents symptomps of *spasticity*, characterized by stiffness in muscles and joints, range of motion exercises should be effected at least twice a day [19, 20]. At the end of this first phase, the focus is moved on strengthening the upper limbs, when possible, to improve patient's independence. In this case, the rehabilitation can involve weights, resistance exercises and electrical stimulation [19]. In fact, even if the communication between muscles and nerves is compromised at the spinal cord level, the neuromuscular system is actually not damaged after that point. An example of electrical stimulation rehabilitation technique is provided by the FES. It involves a current induction in these intact nerves, generating a muscle contraction. Usually, stimulation is obtained by placing large electrodes on the skin area above the muscle of interest [21, 2].

The first acute phase of the spinal cord injury condition is progressively followed by a chronic stage. The rehabilitation exercises during this period must focus on reaching independent ambulation for paraplegic patients. Assistive technologies as *Reciprocating Gait Orthosis* (RGO) support in reducing patient's weight while walking, increasing muscle mass; FES is exploited to create hybrid orthosis and neuroprosthesis, proved to improve ambulation performances [19, 21]. Upper limbs can be rehabilitated as well by means of electrical stimulation, leading to a better functionality [19].

1.2.1 Functional Electrical Stimulation For Spinal Cord Injury

The voluntary contraction of an healthy subject's skeletal muscle is generated in the brain, where an electrochemical signal is sent along the nervous system through nerves, ending on a motor neuron. A motor unit is the ensemble of one motor neuron and its innervated muscle fibers. FES rehabilitation technique can be used only if the motor unit is uncompromised, since it induces a current in the motor neurons of interest making the fibers to twitch and the muscle to contract [19, 2], producing functional body movements like grasping or cycling [22]. In figure 1.2 a comparison between a voluntary and a stimulated contraction of the quadriceps and harmstrings muscles is shown. The same leg movement is achieved in both cases.

Muscle fibers present two main different behaviours regarding the velocity at

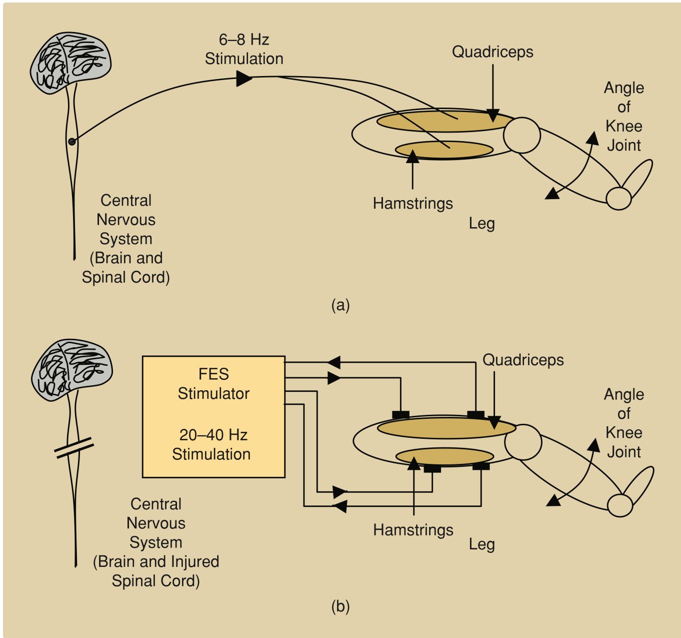

Figure 1.2: **Comparison between a voluntary and a stimulated contraction of the quadriceps and harmstrings muscles.** Reprinted from [2].

which they twitch after the impulse and their fatiguability, making it possible to outline two main classes [2]: fast-twitch and slow-twitch fibers. The fast-twitch fibers present a higher tendency to fatigue, responding quicker to the stimulation signal. The slow-twitch fibers on the contrary, take more time to react to a stimulus but present more endurance with respect to fatigue. The quantity of the two types of fibers forming a muscle is not fixed, but it depends on the kind of exercise that the muscle usually undergoes. Therefore, a prolonged immobility, as in the case of the spinal cord injury condition, could lead to an increase of fast twitch fibers, hence leading to an easy fatiguability and muscle atrophy of the subject. The functional electrical stimulation can reverse the atrophy tendency by strengthening the muscles [2].

In order to stimulate motor units, the electrical stimulation is achieved by means of electrodes, that can be non-invasive, if they are placed on the skin, or invasive, as in the case of percutaneous and epimysial electrodes (placed inside the muscle fibers or on the muscle surface, respectively). Stimulation parameters, as pulse amplitude, duration and frequency, are crucial to achieve a correct rehabilitation [2]. As regards the stimulation frequency, it is really important to consider that there is a different recruitment order of the muscle fibers for stimulated contractions with respect to voluntary ones. In fact, the central nervous system is able to activate different motor units in a specific order, making the contraction more effective in terms of power consumption and fatiguability. FES on the contrary, recruits all the motor units inside the electrode stimulation area at the same time [2, 23]. Furthermore, the stimulation frequency must be in the 20-40 Hz range in order to achieve a FES contraction, while for the central nervous system 6-8 Hz are sufficient [2].

FES induces a higher level of fatigue on the muscle with respect to a voluntary contraction. Indeed, other than the higher stimulation frequency, the electrical stimulation is proved to activate fast-twitch motor units more easily with respect to the central nervous system recruitment order. The characteristic of inverse-order recruitment of electrical stimulation is known as the "reverse size principle", due to the fact that fast-twitch motor units are innervated by large diameter nerves that result to be more electrically excitable even if more fatiguable than the *slow-twitch* fibers [2, 23]. When the electrical stimulation is achieved by non-invasive electrodes, there is no way to avoid the induced higher level of fatigue [2].

1.3 Muscle Fatigue In Spinal Cord Injury Rehabilitation

Induced muscle fatigue is an actual limitation to FES rehabilitation exercises, because it imposes a maximum task duration. After a while, the muscle is no more able to perform an effective contraction as a result of fatigue [22]. Modern research is focusing mainly on four strategies [24]:

- Precise stimulation electrode placement, in order to stimulate specific motor units
- Setting of proper stimulation parameters
- Designing optimized exercise protocols
- Considering a fatigue feedback in order to optimize motor units recruitment

A great advance in FES-based phisioterapeutic systems would be introduced by providing a fatigue estimation feedback. This would lead to a fundamental improvement towards a safer and more stable rehabilitation process [25], since injured patient are not able to provide a sensory fatigue feedback due to their condition [26]. Moreover Shields et al. [27] proved that, by including in the stimulation loop this kind of feedback, it can be possible to improve the stimulation performance of the contraction. Research is working on effective methodologies to integrate a muscle fatigue feedback system into a functional electrical stimulation rehabilitation protocol [26, 23], by highlighting its importance in spinal cord injured patients treatment.

In this thesis, *Micro Electro-Mechanical System* (MEMS) microphone technology is proposed as a tool for muscle fatigue detection. A complete muscle fatigue feedback system based on *BITalino Plugged Board* and MATLAB processing is described, by providing details on its design, assemblage and final validation. The obtained results demonstrated that the system is able to detect fatigue parameters trends during training protocols, making it suitable for future investigation on stimulated contractions.

Chapter 2

State of the Art Of Muscle Fatigue Assessment

2.1 Torque Analysis

The definition of muscular fatigue for a static contraction is often given as the impossibility to maintain the same output force indefinitely in time. For a dynamic contraction the definition involves the output power [28]. Thus, in order to assess fatigue development, one possibility is to measure the torque generated during the muscle movement, which is directly related with the output force. Lindström et al. [3] studied the endurance of thigh muscles measuring the output torque by means of a dynanometer. The development of fatigue is shown in figure 2.1, as a decrease in peak torque at each contraction. During electrical rehabilitation of injured patients, the output torque is important as fatigue feedback. However, there is still a lack of suitable torque sensors for dynamic movements, since the typical rehabilitation exercises that FES induces in subjects (e.g. walking, grasping [22]) can affect the torque measuring by introducing motion artifacts. Moreover, torque sensors are not efficiently wearable for a dynamic recording. Therefore, further research effort is focused on alternative fatigue-related signals, such as *Electromyogram* (EMG) and *Mechanomyogram* (MMG), able to provide an indirect torque estimation bypassing torque measurement [23, 29].

2.2 Electromyography

The electromyography signal represents the electrical depolarization of the muscle fibers. The signal carried by the motoneuron axon is transferred to the muscle fiber, where it propagates from the innervation zone to both fibers extremities. This electrical signal, usually named motor unit action potential, can be acquired by invasive

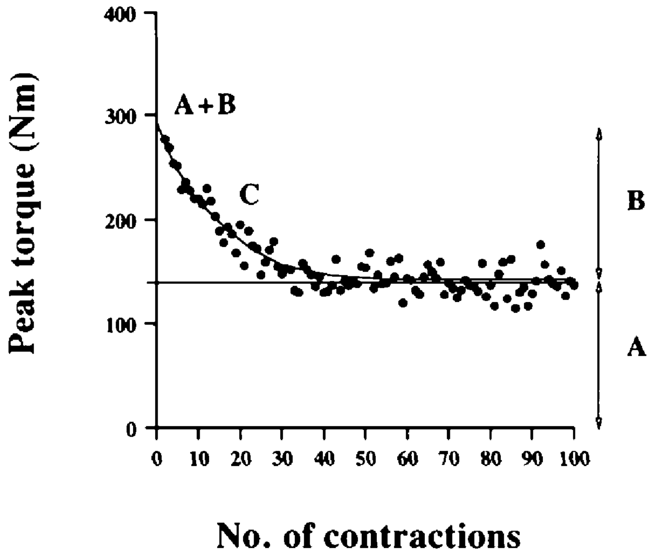

Figure 2.1: **Torque trend in time during fatiguing cycling exercise.** A, B and C are extracted parameters, not debated in this work. Reprinted from [3].

techniques, as intramuscular needles, or non-invasive ones by means of surface electrodes placed on the skin. In the latter case, the distance between the signal source (the muscle) and the recording electrodes introduces a certain number of issues, such as a low pass-filter caused by interposed tissues and a possible common mode interference. Moreover, the EMG signal recorded by surface electrodes is characterized by a lower specificity in recognizing motor units action potentials, due to the fact that the considered muscle volume is bigger than in the case of intramuscular needles. In order to overcome these limitations by keeping the simplicity of use, the bipolar differential configuration is usually preferred. This involves two recording electrodes referred to a reference one [30].

The non-invasive EMG technique is widely used for investigating the muscle physiology nowadays, due to its ease-of-use and provided information. In particular, from EMG raw signal it is possible to extract time and frequency domain parameters, whose in-time trends reflect the muscle fatigue evolution [31]. Figure 2.2 shows the output trends of force and mean frequency of EMG signals during an isometric contraction of one hand muscle. The term *isometric* indicates a static contraction that does not involve muscle shortening. The subject is not able to maintain the initial output force indefinitely in time: from the "failure point" on, it tends to decrease. Observing the EMG frequency-domain parameter, it starts to decrease from the very beginning of the contraction, proving its ability to describe muscle fatigue along the entire exercise, presenting evident parameters trends.

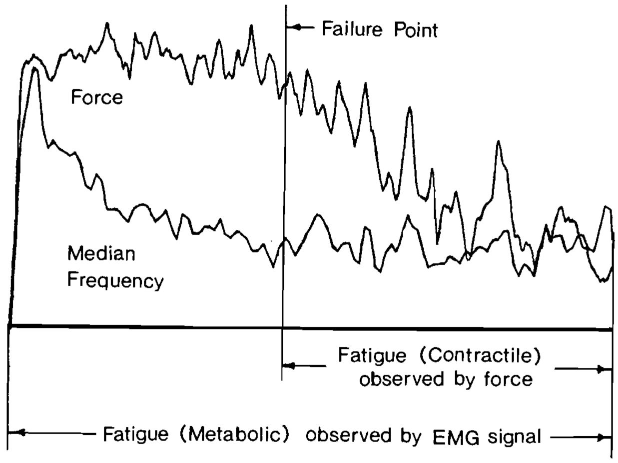

Figure 2.2: **Output force and electromyogram mean frequency measured during an isometric contraction of the first dorsal interosseus hand muscle.** Reprinted from [4].

EMG fatigue parameters are usually investigated during isometric, constant force voluntary contractions, as this condition simplifies the analysis. Dynamic contractions, inherently involving muscle shortening and thickening, present the need to identify artifacts on the EMG caused by the continuous relative motion between the muscle fibers and the surface electrodes [30]. In fact, the positioning of the electrodes is of fundamental importance in EMG recording since the signal is highly affected by this factor [31]. Furthermore, the surface electrodes positioning imply a preparation of the skin, consisting in a gently scrubbing and cleaning of the area, in order to guarantee an optimum contact [32, 33]. This strategy reduces the electrical noise produced by transducer-skin impedance [31]. Over and above practical considerations, the signal frequency content may rapidly change in time during dynamic contractions. Therefore, it also requires more suitable signal processing techniques such as time-frequency distributions or wavelets [30]. As regards SCI rehabilitation, the myoelectric signal is able to assess muscle fatigue during static [34] and dynamic [32] FES induced contractions, presenting evident parameters trends. However, the electrical stimulation requires a blanking strategy for EMG signal amplifiers since the amplitude of stimulation pulses produces a significant artifact [35, 25, 34, 32].

2.3 Mechanomyography

The mechanomyography signal is an expression of the mechanical activity of the muscle. During a voluntary contraction, the central nervous system activates muscle fibers in a certain order, to make the contraction more effective in terms of energy consumption and fatiguability [2, 23]. This recruitment order involves then a non-synchronous twitch of the muscle fibers. Whenever a muscle fiber twitches, it shorthens and thickens generating a pressure pulse [36], even during an isometric contraction where the length of the whole muscle is not changing [30]. Moreover, the movement of the muscle is not perfectly symmetric, also because of the different thickness of muscle fibers and other tissues along the limb. This produces further pressure waves [36]. The summation of all these pressure pulses can be sensed on the skin surface by means of different tranducers, such as piezoelectric contact sensors, accelerometers, laser distance sensors and condenser microphones [36, 37]. The signal acquired by these transducer is called mechanomyogram, that represents the tranverse displacement of the skin [36, 37].

Mechanomyography presents some benefits with respect to EMG. First, the placement of MMG transducers is not a crucial element as for electromyography, because of the propagation of the pressure waves along the muscle. Thus, a precise recommendation for mechanomyography sensor placement is not available, as it does not highly influence the resulting signal. As regards preparation of the skin, for the mechanomyographic signal is not required [37, 38], differently from the electromyographic one that is very sensitive to skin impedance variations due to sweating [31]. Moreover, MMG signal is suitable for muscle properties analysis during electrical stimulation techniques, such as functional electrical stimulation. In fact, it does not present a stimulation artifact during recording, while EMG signal requires blanking strategies [35].

Mechanomyography signal is investigated in research for different applications, such as muscle machine interfaces and prosthesis control [37, 35, 31], motor units behavior analysis and monitoring of muscles properties during physical activities [37]. In particular, MMG signal is able to represent muscle fatigue development [31, 36], also during electrically stimulated contractions [39] such as the ones provided by FES techniques [29]. The MMG signal suitability as fatigue feedback control during electrical stimulation on spinal cord injured patients has been tested by Krueger *et al.*. The analysis of amplitude and frequency parameters showed a significant difference between healthy and injured subjects, showing the typical atrophism and increase of fast-twitch fibers in the latter. The signal is therefore able to characterize muscle properties such as muscle fibers composition and fatiguability.

As the EMG signal, MMG is able to provide an indirect torque feedback during an isometric contraction in order to simplify the acquisition set-up [29]. In fact, as already stated, torque sensors are not suitable for certain movements and tasks.

Mechanomyography can be also used for dynamic contraction measurements, taking into account the non-stationarity of the signal. In fact, as in the case of the electromyography, the distance between the transducer on the skin and the muscle fibers is not fixed during a dynamic exercise, as well as muscle length. These factors can contribute to rapid changes in the signal amplitude, requiring more recent and reliable signal processing tools [35].

2.3.1 MEMS Condenser Microphones

One of the possible transducers for MMG is a condenser microphone. In this thesis, MEMS condenser microphone were selected because of their suitability during dynamic movements, the high integrability and small dimensions [40]. In fact, Posatskiy *et al.* [41] tested the motion artifact in the mechanomyography signal recorded by a condenser microphone, proving its robustness. When compared to an accelerometer transducer, the mechanomyography signal recorder by the microphone signal showed less artifacts of limb movements [42], resulting more reliable during daily-like rehabilitation exercises. When thinking of SCI rehabilitation, the possibility of inducing these kind of movements is very important. Typical FES exercise in fact contemplate exercises such as grasping and cycling [22].

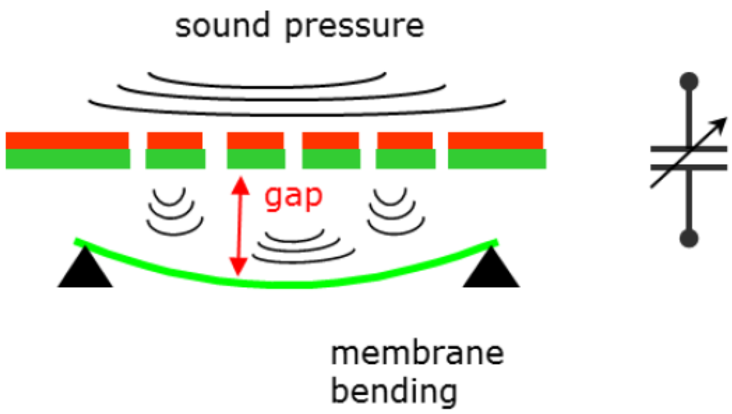

Figure 2.3: **Working principle of a MEMS condenser microphone.** The sound pressure generates a vibration on the movable capacitor plate. The fixed plate is pierced in order to allow the air flow. The resulting component is a variable capacitance. Reprinted from [5].

MEMS condenser microphones acoustic transducers are able to sense pressure waves generated by the displacement of the skin. The working principle of a MEMS condenser microphone is shown in figure 2.3. The main component is a capacitor made of two silicon plates [5, 43], one free to move if excited by a pressure wave, the other fixed. The latter is pierced in more spots so that the air is able to cross it and reach the movable plate. The air inside of the capacitor area is able to exit because of a ventilation hole [5].

The transducer output is hence a variable capacitance [5]. However, the actual output of a MEMS condenser microphone is the result of an *Application Specific Integrated Circuit* (ASIC), able to convert the capacitante change into an analog output, such as a voltage, or a digital output, expressed more commonly in a *Pulse Density Modulation* (PDM) encoding [44]. In this thesis, two different MEMS condenser microphones have been considered and tested for MMG recording and muscle fatigue assessing. The main difference is that one is an analog transducer, while the other is a digital one. For an analog microphone, the ASIC module is an amplifier, able to bias the microphone output at a specific constant value ranging between ground and the supply voltage. As regards the digital output, the PDM codification is able to represent the audio signal using a single bit digital system, easily reconductable to an analog signal [44]. This is possible using two main modules, the (i) $\Delta\Sigma$ modulator and the (ii) digital/decimation filter [7]. The ensemble of the two modules is shown in figure 2.4.

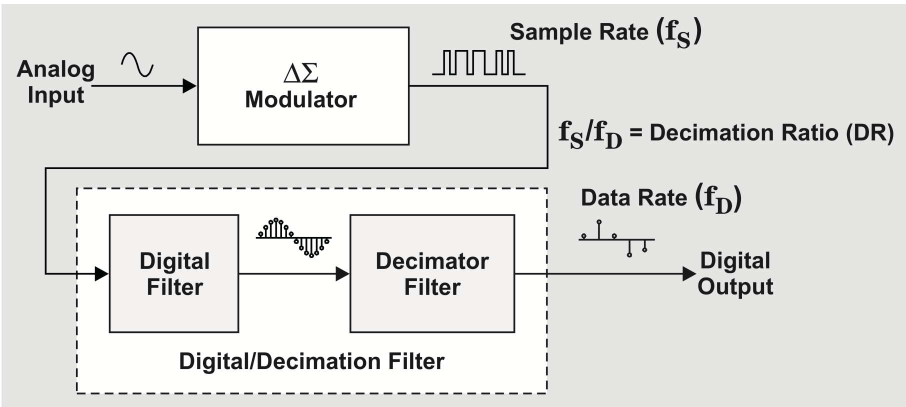

Figure 2.4: **Complete PDM audio trasmission system.** The $\Delta\Sigma$ modulator and the digital/decimation DFSDM modules are shown, along with their outputs when a sine wave is the analog input. Reprinted from [6].

The first module main goal is to oversample the signal, typically to values greater than 3 MHz, and digitize it. By means of a differential amplifier, a certain number of integrators, one 1-bit *Analog to Digital Converter* (ADC) and one 1-bit *Digital to Analog Converter* (DAC) the analog input is converted into a digital, single bit output [7]. The circuit is shown in figure 2.5 along with the resulting PDM output of a $\Delta\Sigma$ modulator when the analog input is a sine wave. The pulse train ranges between 0-1, being a single bit signal.

The second module is called *Digital Filter for Sigma Delta Modulators* (DFSDM),

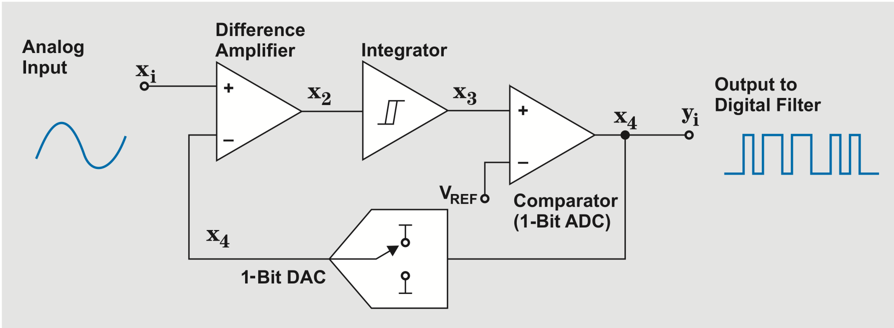

Figure 2.5: **Sigma-Delta modulator circuit.** The main modules of a ΔΣ modulator are shown. The example input signal is a sine wave. The output of the ΔΣ modulator is a pulse train ranging between 0-1, expressed in single-bit PDM. Reprinted from [7].

consisting in a digital/decimation filter. This peripheral is able to generate a clock line, reading the PDM input at every rising egde [45]. The signal is then digitally low-pass filtered, and because the quantization rate corresponds to the clock one, the resulting signal is at high resolution. An example of the output of the low pass filter is shown in figure 2.6. The original signal shape can be recognized, because the low pass filter eliminates the high frequency quantization noise introduced by the ΔΣ modulator.

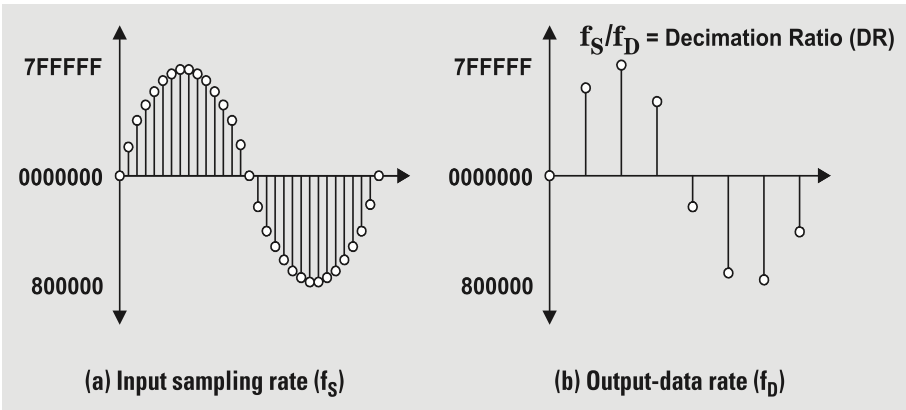

Figure 2.6: **Decimation of a ΔΣ modulated, low pass filtered sine wave.** Left: output high resolution quantized signal from the digital low-pass filter. Right: decimated signal. Both signals have a 24 bit amplitude resolution. Reprinted from [6].

The following step is the decimation, in order to lower the sample rate simplifying the audio trasmission. In fact, the low-pass filter output has a huge number of samples, requiring high computational performances. Moreover, the majority of them is not necessary in order to reconstruct the signal, it is sufficient to comply with the Nyquist theorem. Decimation module discards the unnecessary samples, without losing any information [6]. In figure 2.6 the resulting signal is shown. The DFSDM output is then a n-bit digitized version of the original audio data, often referred to as *Pulse Code Modulation* (PCM) standard for audio transmission [45]. In this way, the signal can be trasmitted and completely reconstructed [6].

2.4 Further methodologies

2.4.1 Sonomyography

A more recent, non-invasive methodology for muscle fatigue assessment is the sonomyography. In fact, ultrasound images can be used to observe the change in muscle thickness during a fatiguing contraction [31, 46]. Shi *et al.* [46, 47] proved the ability of sonomyography to assess muscle fatigue development during an isometric contraction of the biceps muscle, comparing this parameter trends with EMG amplitude and frequency parameters an torque signal. This technique is usually used as a completion of EMG or MMG signals [31].

2.4.2 NIRS

During a fatiguing contraction, two main factors drive the oxygen flow inside the muscle. First, the contraction prevent the blood to flow freely, and that causes a decrease of oxygen volume. On the other hand, the muscle requires oxygen during the contraction, thus the blood flow is increased in the muscle area. These changes in oxygen and blood flow can be sensed at the skin in a non-invasive way, using *Near Infra-Red Spectroscopy* (NIRS). The working principle is based on the different infrared light absorption of deoxygenated and oxygenated haemoglobin at a wavelength equal to 760 nm, while at 800 nm the absorption is the same for both kinds of heamoglobin. By analyzing light absorption at the two different wavelength, it is possible to assess the muscle oxygenation. This technique can be used for studying oxygen changes during a fatiguing exercise [31]. Muramatsu *et al.* [48] introduced a NIRS probe in a wearable muscle suit support system, proving its ability to estimate muscle fatigue changes. However, this methodology has been proposed just for healthy muscle fatigue analysis, thus more research is needed for further insight [31].

Chapter 3

Materials and Methods

3.1 Mechanomyography sensors

Among the different possible techniques introduced in the previous chapter, the mechanomyography sensors were chosen to develop the experimental part of the thesis. The mechanomyography signal is recorded by acoustic transducers, which have been demonstrated to be suitable tools for analysis during dynamic movements [49], such as the ones induced during spinal cord injury rehabilitation. MMG transducers are also characterized by easy-placement, as the signal is not influenced from the sensor location on the skin. Besides, they are not affected by electrical stimulation artifacts. Therefore, they result to be suitable for being employed in SCI rehabilitation, where electrical stimulation is used to induce limb movements. According to this, the perfomance and peculiar characteristics of digital and analog microphones were compared. Experiments were carried out by acquiring MMG signal with two different microphone-based systems: (i) MEMS digital microphone integrated on SensorTile and (ii) MEMS analog microphone driven by Bitalino system. In the following sections the features of both the acquisition systems will be described.

3.1.1 MEMS Digital Microphone Integrated on SensorTile

During SCI rehabilitation it is interesting to collect several different information about the status of the limb under exercise [14]. The aim of this study is to analyze muscle fatigue particularly, but mechanics and orientation data could be elements of interest thinking of a more complete rehabilitation system. This study focuses on the analysis of the muscle fatigue, by using the STMicroelectronics SensorTile Development Kit. This system has been selected keeping in mind the idea of a final rehabilitation system where also mechanical and orientation information could be interesting elements for the therapist.

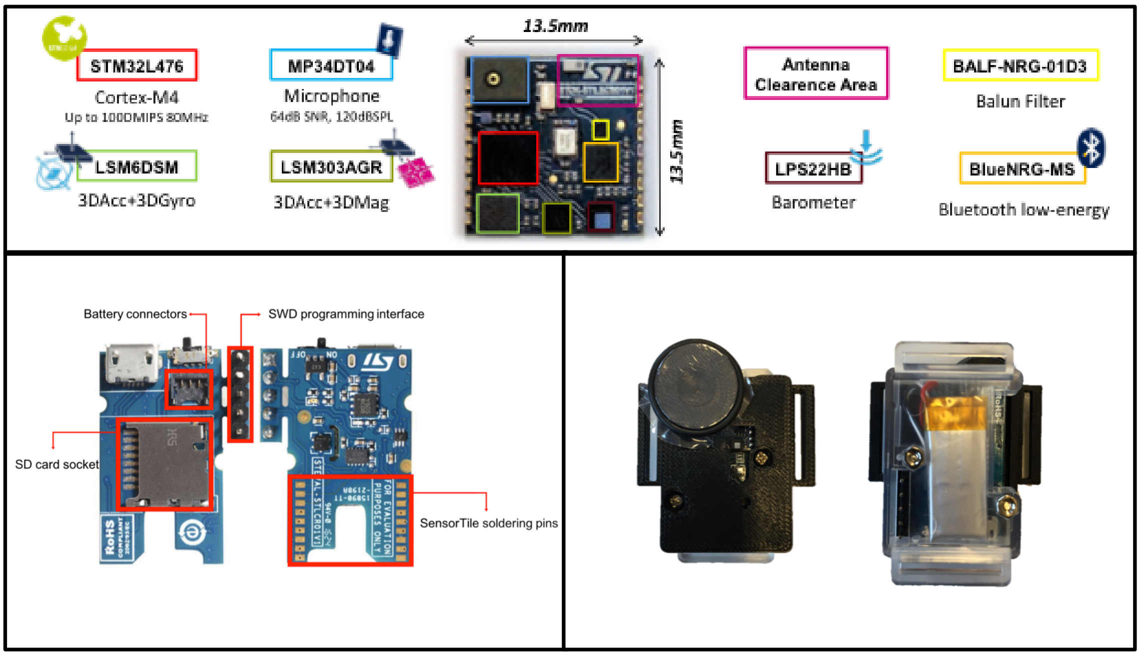

Figure 3.1: **SensorTile module overview.** Top: SensorTile components description. Reprinted from [8]. Bottom left: Cradle board. Reprinted from [9]. Bottom right: SensorTile module for Mechanomyogram sensing (front and back).

SensorTile is a commercially available integrated development platform, designed for wearable applications. The module is able to record various kind of signals, including acceleration, angular speed, orientation and atmospheric pressure [8]. In particular, it presents a MEMS condenser digital microphone. The complete set of *SensorTile* sensors is shown in table 3.1, while the module is shown in figure 3.1.

SensorTile sensors

Sensor	MEMS Digital Microphone	Inertial Module	e-Compass module	MEMS pressure sensor
Model	MP34DT04	LSM6DSM	LSM303AGR	LPS22HB
Manufacturer	*ST Microelectronics*			

Table 3.1: *SensorTile sensors [8].*

The SensorTile module was soldered on a cradle board as shown in figure 3.1, to provide the power supply through a 100 mAh Li-Ion battery and to make it wearable. Furthermore, it offers a micro-SD card socket so that the recordings from the sensor can be locally saved. The on-board ARM 32-bit microcontroller (STM32L476) is flashed with an *Open Development Environment* (ODE) function package provided by STMicroelectronics [50]; hence, the user can interact with the SensorTile module by using a dedicated smartphone application named *STBlueMS* (available for Android and iOS devices). The *SensorTile*-based system and the smartphone communicate via Bluetooth technology.

The mechanomyogram signal recorded during a muscular activity presents a low frequency bandwidth (2-120 Hz [38]). The condenser digital microphone integrated on SensorTile is designed for vocal application, therefore there is no information about the frequency response below 100 Hz in the datasheet. For this reason, different tests were carried out to characterize the performance of the microphone in the range of frequencies of interest. To this end, the digital microphone was provided with an 3D printed acoustic chamber (conical, 10 mm $\varnothing$, 6 mm height) designed with SolidWorks software, integrated in the SensorTile plastic case (see section 3.2). The chamber was sealed at the bottom to the microphone with *Polydimethylsiloxane* (PDMS), while the top was covered by a 23 μm thick Mylar membrane, as shown in figure 3.1. The SensorTile module was then tested inside the Politecnico di Torino *Dipartimento di Energia* (DENERG) anechoic room. It must be noted that the anechoicity of the room is guaranteed above 100 Hz, therefore not in the low frequency range of interest. Tests were still performed, considering the anechoic room a more controlled environment than an ordinary room.

The setup for the microphone characterization analysis is shown in figure 3.2. A calibrated NTi XL2 *Sound Level Meter* (SLM), accessorized with a measurement microphone (MA220 Preamplifier, M2211 capsule) stood on a tripod, facing a NTi TalkBox *Reference Sound Source* (RSS). The distance between the microphone capsule and the TalkBox membrane was 30 cm. The SensorTile module was fixed at the bottom of the measurement microphone, with the top of the acoustic chamber facing the TalkBox. The first test consisted in recording the background noise of the room, without using the RSS. Then, the following standard sounds were generated by the TalkBox:

- White noise (60dBSPL@1m)
- Male Speaker (English, 60dBSPL@1m)

The characterization results are depicted in figures 3.3a, 3.3b and 3.3c. It is evident that the digital microphone is actually able to sense low frequency sounds, even if an attenuation is present with respect to the SLM. It is evident that the

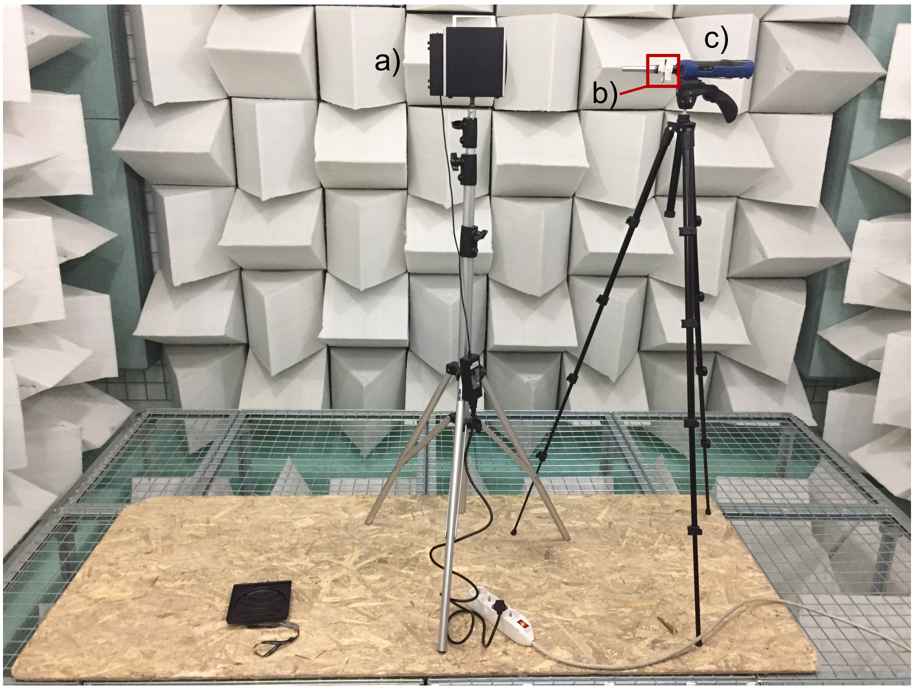

Figure 3.2: **Anechoic room setup.** a) NTi TalkBox Reference Sound Source, b) SensorTile module, c) NTi XL2 Sound Level Meter.

digital microphone can sense low frequency signals, even if an attenuation is present in the range 10-60 Hz with respect to the SLM and below 10 Hz no power is detected.

In light of the results, and considering that the main power frequency of MMG is above 10 Hz in fatigue analysis contractions [38], the digital microphone integrated on SensorTile was assessed to be suitable for the application.

Further considerations on the MEMS digital microphone can be performed as regards its sensitivity. From technical documentation [51] the sensitivity is indicated equal to –26 dBFS. In order to physically interpret digital microphone output values, expressed over 16 bit full scale, it is necessary to indicate a sensitivity expression able to convert the digital level into applied pressure (Pascal). In the following paragraph, an interpretation of the digital microphone sensitivity is proposed.

$$Sensitivity_{dBFS} = 20 * log_{10}(\frac{Sensitivity_{FS}}{Output_{DREF}}) \tag{3.1}$$

In equation 3.1, reprinted from [52], $Sensitivity_{FS}$ is the sensitivity expressed as a percentage of the full-scale output that is generated by a 1 Pa pressure input and $Output_{DREF}$ is the full-scale digital output level. $Sensitivity_{dBFS}$ represents the sensitivity as expressed on the microphone datasheet, equal to -26 dBFS as already

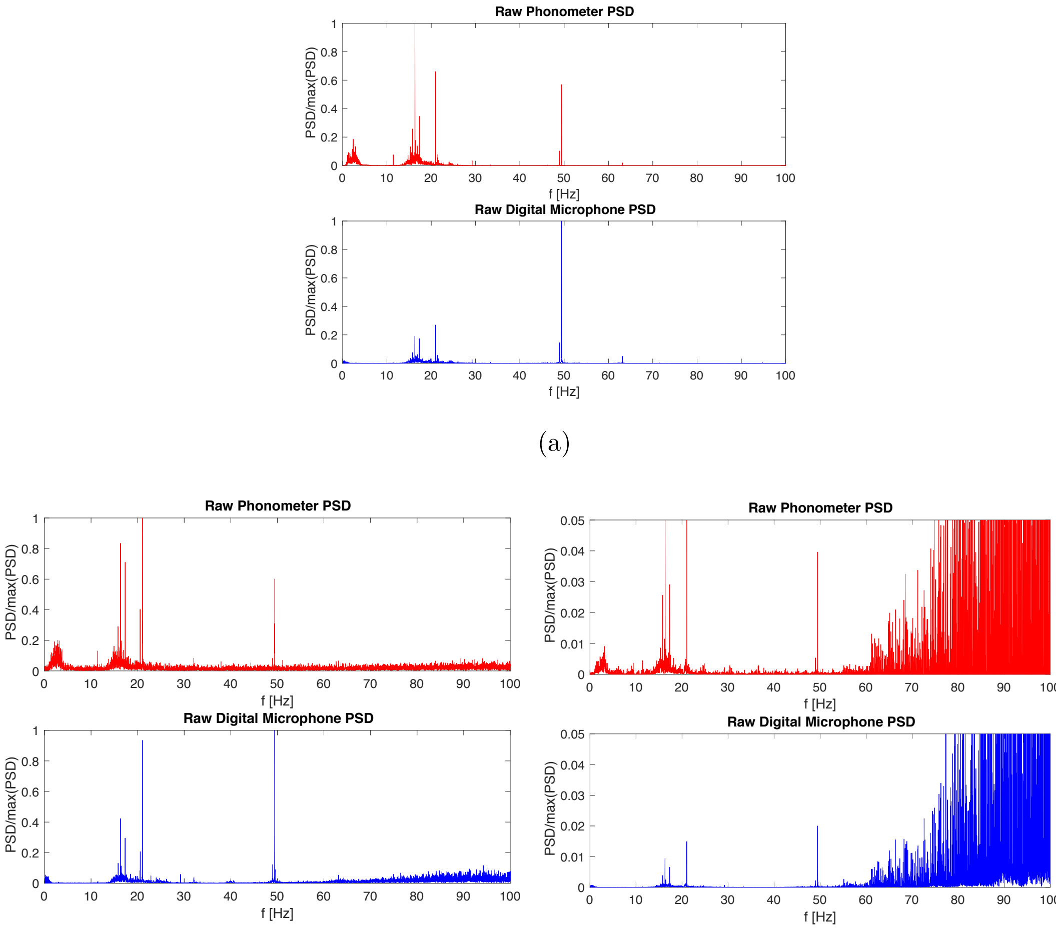

(a)

(b)

(c)

Figure 3.3: **Comparison between phonometer and digital microphone PSD.** a: background Noise. b: white noise. c: male voice speaker.

stated.

$$-32767 = -2^{16}/2 < x < -2^{16}/2 = 32767 \tag{3.2}$$

$$Output_{DREF} = 2^{16} - 1 = 65535 \tag{3.3}$$

$Output_{DREF}$ can be easily assessed, as the microphone output is a 16 bit digital level. Thus, the output range for the digital microphone is the one described in equation 3.2. The full-scale digital output level is shown in equation 3.3.
Inverting equation 3.1, it is possible to compute the $Sensitivity_{FS}$ value, equal to 3276,5, expressed in digital level over Pascal. The computation of the $Sensitivity_{FS}$ value enables the conversion of the digital microphone output into Pascal values.

3.1.2 MEMS Analog Microphone

Up to now, it is not available a commercial sensor for MMG recording [14]. The *SensorTile* digital microphone performance were hence compared with a Knowles MEMS condenser analog microphone (SPU1410). This acoustic sensor has been selected since it already proved suitable perfomance in low frequency applications [53], [14]. It is, in fact, characterized by a flat frequency response in the range of 10-100 Hz [54]. Its sensitivity is -38 dBV/Pa (corresponding to 12.56 mV/Pa).

The *Printed Circuit Board* (PCB) for the MEMS microphone was designed with Altium software following the indication provided by Woodward *et al.* [14] and it was realized by the *Atelier de Fabrication de Circuits Imprimés* (ACI) at *École Polytechnique Fédérale de Lausanne* (EPFL). The Altium design is shown in figure 3.4, along with the realized PCB. The diameter is 7 mm, while the dimension of the pads was set based on the producer recommendation [54].

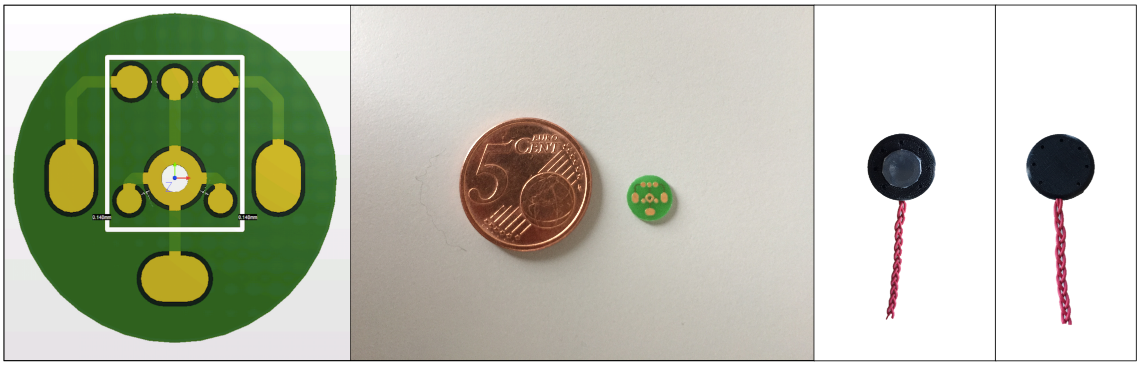

Figure 3.4: **Analog microphone overview.** Left: PCB Altium design, showing microphone footprint. Center: final PCB. Right: complete analog microphone sensor for mechanomyography (front and back)

The microphone soldering on the PCB was achieved using a proper MEMS soldering instrumentation, shown in figure 3.5. The microphone and the PCB were carefully aligned, then the temperature profile was set based on the producer recommendation [54] (see Appendix figure 6.4). Finally, three common wires were soldered to the oval pads, in order to power the microphone and record the MMG signal.

In order to realize a sensor suitable for rehabilitation, it was necessary to realize a 3D printed plastic case, based on the one made by Woodward [14] and described in section 5.2. The complete sensor is shown in figure 3.4; a 23 μm thick Mylar membrane was placed on the top of the acoustic chamber (see section 3.2) integrated in the plastic case.

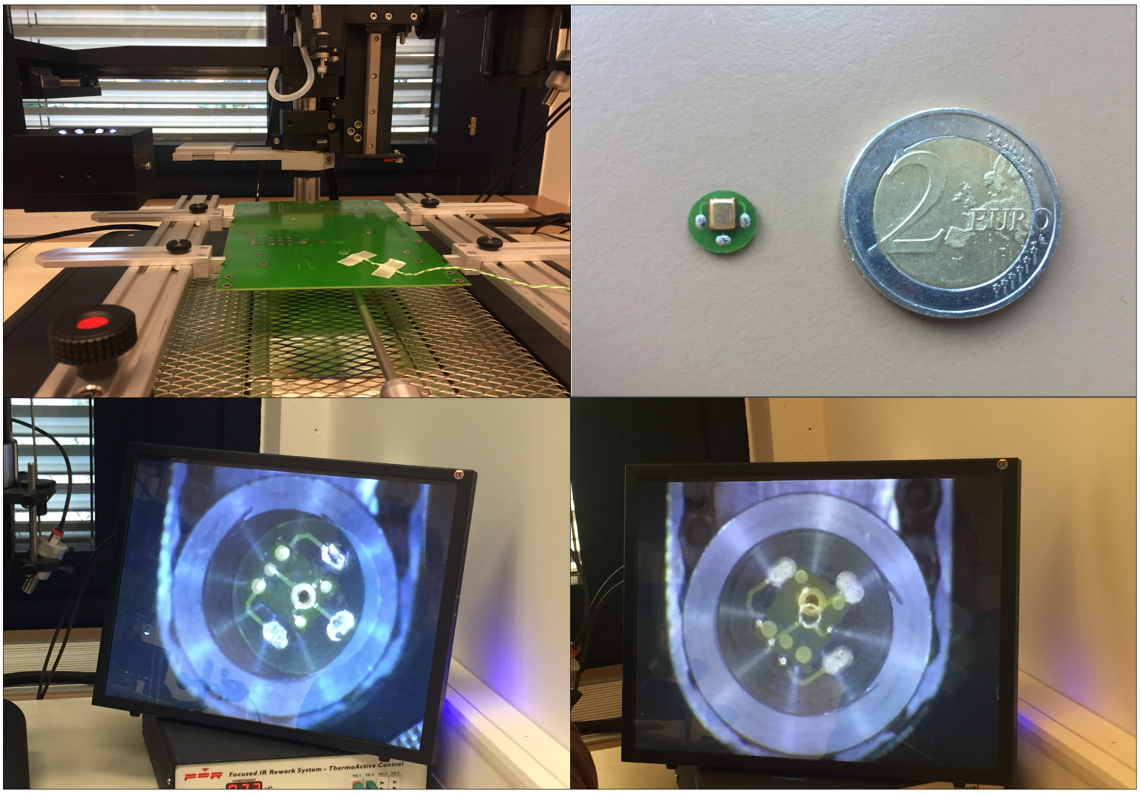

Figure 3.5: **Microphone soldering setup and result.** Top left: soldering instrumentation. Top right: final PCB with soldered microphone. Bottom: alignment process showed on a monitor.

3.2 3-D Printed Acoustic Chamber

The realization of a suitable acoustic chamber for a MMG microphone is an important element. In fact, the interposed air inside of the chamber transfers the mechanical vibration of the skin to the condenser microphone. The shape and size of the acoustic chamber can influence the the MMG signal detected [49], in particular in terms of gain at the MMG low frequencies [53].

An optimized acousting chamber was realized by the *Atelier de Fabrication Additive* (AFA) at EPFL for MMG recording in line with literature investigation [49], [53]. In fact, Posatskiy *et al.* [53] demonstrated that highest gain is obtained by using a conical acoustic chamber with respect to a cylindrical one with a Knowles SPU1410 MEMS analog microphone. According to this study, the best configuration was found to be a conical chamber (5 mm height and 7 mm diameter) with 4μm thick aluminized Mylar membrane applied on the top. For this reason, we used the same acustic chamber dimensions for both the analog and digital microphones.

However, due to the unavailability of an identical Mylar membrane, the one used in this work was a not aluminized, 23 μm thick. The base of the chamber was sealed to the microphone by means of a PDMS layer.

The Appendix section shows the design of the 3D printed (material: black *Acrylonitrile Butadiene Styrene* (ABS)) acoustic chambers integrated in the plastic cases for both of the microphones (figure 6.1 and figure 6.2).

3.3 Hardware Implementation

BITalino Plugged Board is the core of the recording system. It is controlled by a MATLAB®algorithm running on a MacBookAir laptop, that set all the recording parameters via Bluetooth transmission.

For the validation of the system, the following sensors were employed:

- EMG module (BITalino kit)
- MMG analog microphone module
- MMG SensorTile module

The EMG and the MMG analog microphone modules are managed by BITalino, with a sampling frequency equal to 1000 Hz. The BITalino board is powered by a rechargeable Li-Po Battery (500mAh), and in turn it provides a 3.3 V voltage for the MMG analog microphone module powering. The MMG signal was pre-amplified 2.77 times, using the amplification circuit in figure 3.6. The amplification stage consists of a non-inverting amplifier (LMC6482, Texas Instruments) and two resistors (10 KΩ and 18KΩ). The obtained voltage resolution, considering that the ADC resolution of both channels is 10 bits, is equal to 1 mV. As regards the EMG signal, it is pre-amplified 1000 times by the amplification stage integrated on the BITalino kit sensor module (the complete transfer function is provided by [55]).

On the other hand, the *SensorTile* module is not managed by the BITalino board. A dedicated application for smartphones, called *ST BlueMS*, was used for starting and stopping each recording, saving data on a Samsung SD card, and sampling the signal at 8000 Hz. The application is easy-to-use, providing a *Graphical User Interface* (GUI) where the user can manage the recording and insert instructions. The plugged-in code of the SensorTile ARM microprocessor was slightly modified, by using the Eclipse-based SW4STM32 *Integrated Development Environment* (IDE) and a ST-LINK/V2 programmer. The original instructions to manage the microphone recording were long, case-sensitive words (e.g. "AudioStart"). In order to simplify the recording management, they were replaced by "a" to start the recording and "s" to stop it. The code was modified also for changing the digital status (on/off) of

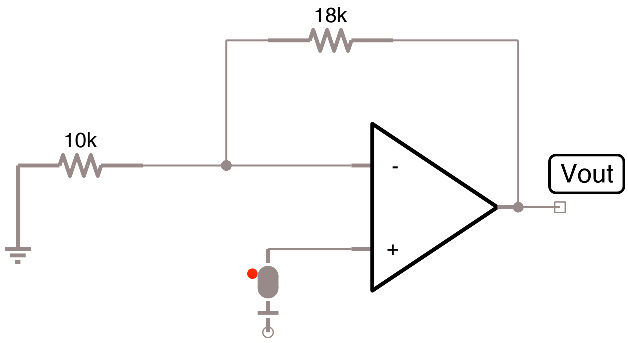

Figure 3.6: **Pre-amplification circuit for MEMS analog microphone.** Components: one non-invertent amplifier (LMC6482, Texas Instruments) and two resistors (10 KΩ and 18KΩ).

the SensorTile board pin nr#12 during the acquisition. This pin has been used for the synchronization of the acquisition signals. In fact, it is very important for the analysis that the signals from all sensors are synchronized. Therefore, the BITalino has been connected to this pin to record the on/off signal, that appears as a port signal ranging between 0-3.3 V. As described in section 5.4 describing signal processing, the EMG electrodes and the MMG analog sensor module data are considered only in the time range where the SensorTile module was actually recording. The complete recording system is shown in figure 3.7.

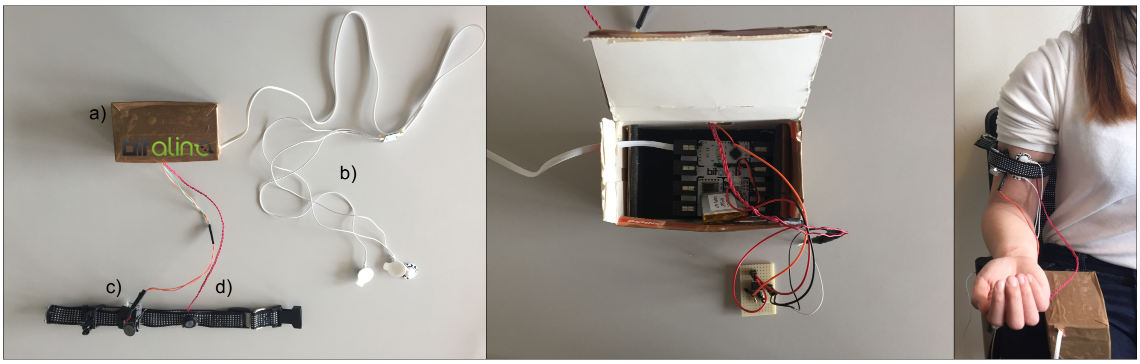

Figure 3.7: **Complete fatigue monitoring system.** Left: a) BITalino-based recording station, b) EMG electrodes, c) SensorTile for MMG recording module, d) analog microphone module. Center: BITalino Plugged Board connected to the analog microphone pre-amplification board. Right: complete system setup on the biceps brachii muscle.

3.4 Signal Processing

In this section the signal processing used to obtain muscle fatigue parameters from three different sensors is described. In order to observe a change in a muscular signal (e.g. EMG, MMG) in time and frequency content, three parameters were extracted from each 2-seconds window:

- *Average Rectified Value* (ARV)
- *Root Mean Square* (RMS)
- *Mean Frequency* (MF)

Each of these parameters are formally described by equations 3.4, 3.5 and 3.6, respectively [56, 57], where x_i is the signal sample, f_i the frequency axis sample, PSD_i is the power spectral density sample, and n is the number of samples of the signal in a 2 seconds window (equal to 2000).

$$ARV = \frac{\sum_{i=1}^{n} x_i}{n} \tag{3.4}$$

$$RMS = \sqrt{\frac{\sum_{i=1}^{n} x_i^2}{n}} \tag{3.5}$$

$$MF = \frac{\sum_{i=1}^{n} f_i * PSD_i}{\sum_{i=1}^{n} PSD_i} \tag{3.6}$$

The *Power Spectral Density* (PSD) was obtained by means of the MATLAB® function *pwelch*, using a n samples-long hamming window. In fact, this MATLAB® function performs the Welch's overlapped segment averaging PSD estimator. The signal processing window has been selected of 2 second as a compromise between a time period sufficiently short to consider the signal stationary, but long enough to obtain an acceptable frequency resolution (0.5 Hz) when computing the signal PSD.

Before computing the fatigue parameters, the signal was processed following a workflow as shown in figure 3.8. In the workflow *EMG* is the EMG signal, *MMG1* is the MMG signal from the analog microphone, *MMG2* is the MMG signal from the digital microphone, *trigger* is the SensorTile #12 pin signal and *AMB* is the background noise of the room acquired by a SensorTile module completely identical to the one used for MMG recording.

To proceed with the data analysis, it is important to underline that the digital microphone signal presented a switch artifact in the first second, as visible in figure 3.9. This artifact was probably due to the status change of the SensorTile

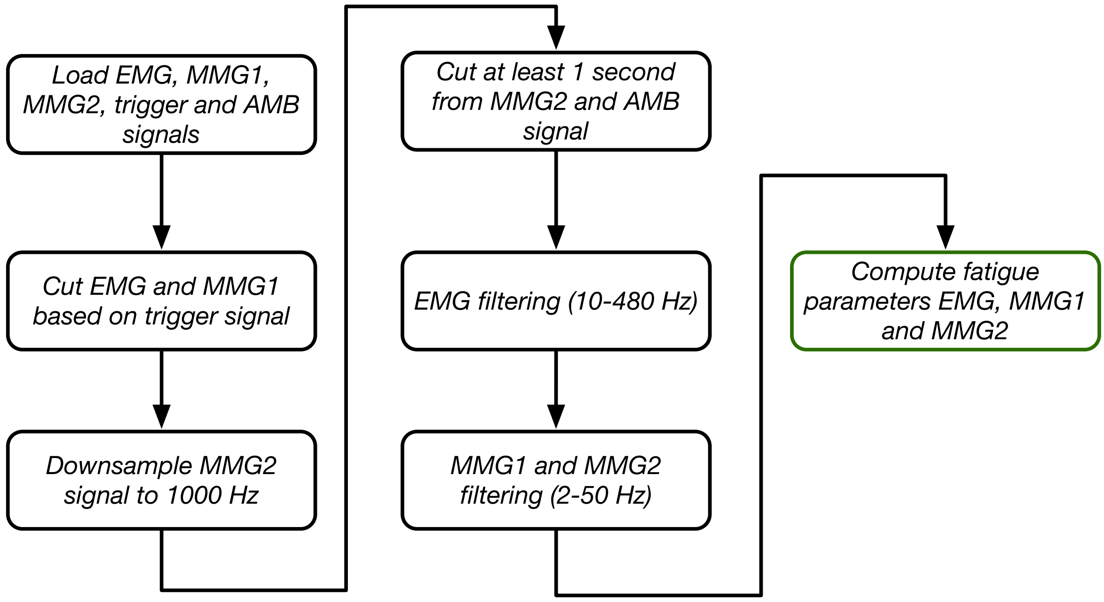

Figure 3.8: **Flowchart of the signal processing algorithm to obtain muscle fatigue parameters.**

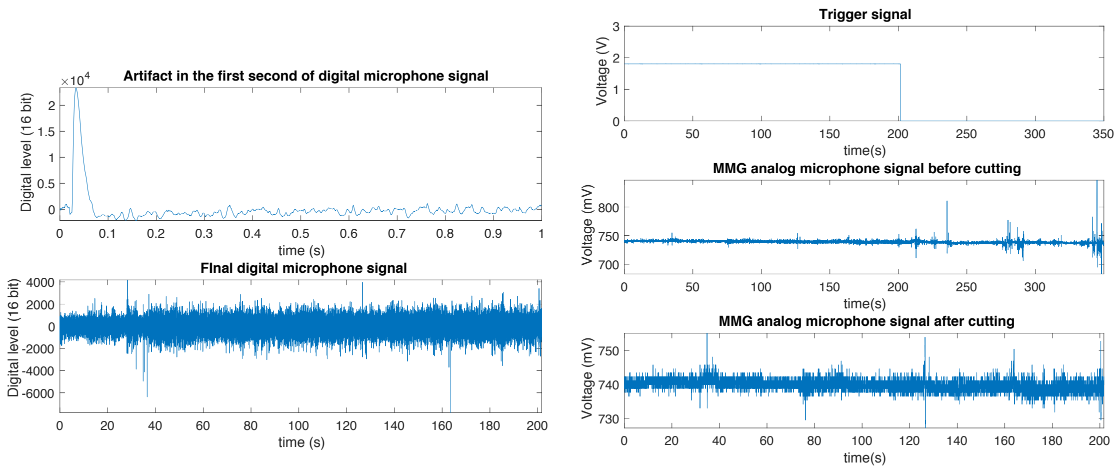

(a) (b)

Figure 3.9: **Editing of signals.** a: cutting of the first second of digital microphone signal because of switch artifact. b: editing of EMG and MMG analog microphone signal based on the trigger generated by the SensorTile module.

nr#12. Therefore, the first second of the signal in the analysis was not included for the analysis. Then, the EMG and the analog microphone signals were edited in a syncronized manner with respect to the trigger signal (figure 3.9). The SensorTile module sampled the signal at 8000 Hz.

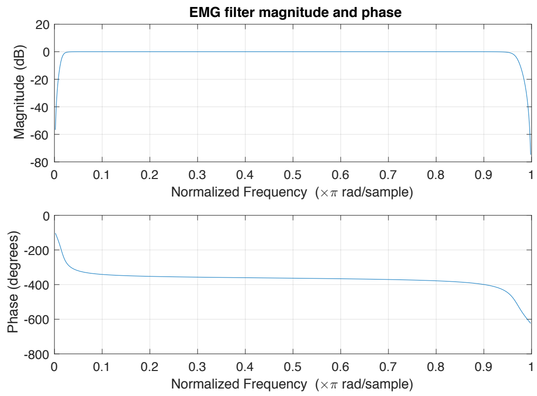

(a)

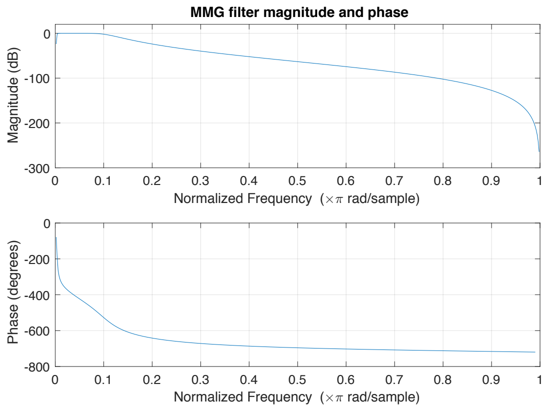

(b)

Figure 3.10: **Filter design.** a: EMG filter (magnitude and phase). b: MMG filter (magnitude and phase).

The digital microphone signal was then downsampled at 1000 Hz to avoid oversampling, as its bandwidth is 2-120 Hz [38]. As shown in figures 3.10a and 3.10b the EMG and the MMG signals were then filtered using a 10-480 Hz and a 2-50 Hz bandpass 3^{rd}-order Butterworth filters, respectively. The frequencies for the bandpass filter range for EMG were set considering the typical values reported in literature [58], [59], [33]. For MMG signal the bandwidth was selected by considering that the main power frequency for an isometric, constant force, biceps contraction is between 10-22 Hz [38]. The validation of the system, as it will be described in section 4, is carried out during this specific kind of contraction. In figure 3.11 it is possible to see an example of raw and filtered MMG signal PSD of a biceps muscle in isometric condition, showing that the majority of the power is below 50 Hz.

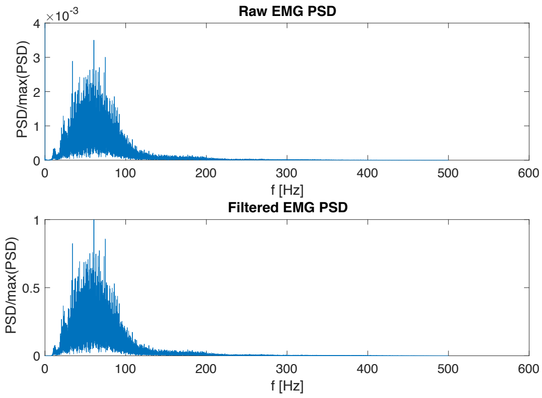

(a)

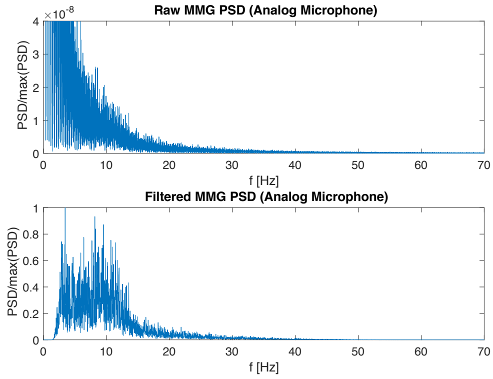

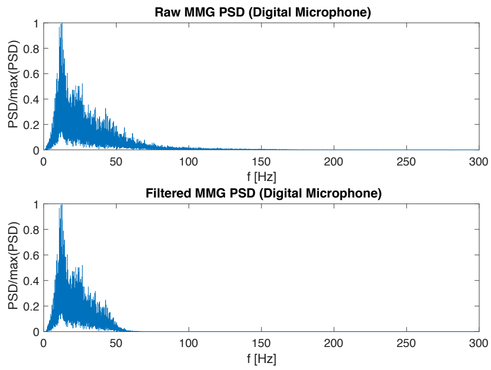

(b) (c)

Figure 3.11: **Signals Filtering.** Resulting PSD of: EMG, b: analog microphone MMG and c: digital microphone MMG after filtering.

The second SensorTile module was included in the validation experiments as a reference for proving the ability of the digital microphone to sense a signal low frequencies signals, hence fatigue estimation. These details will be provided in chapter 4.2. In order to compare the MMG signal and the background noise provided by the SensorTile used as control, the PSD of both of these microphones was computed by means of the MATLAB® function *pwelch*, using a *hamming* window long as one third of the entire signal length, with a 50% overlap. Since the main goal is to show a comparison between the two digital microphones PSD, the window length and the overlapping were selected testing different combinations of values, observing the resulting PSD plot. The final parameters choice corresponds to the plot showing the PSD difference in the most clear way, providing a proper PSD frequency resolution.

Chapter 4

Experimental Validation

In this section the validation of the system realized with MEMS condenser microphones for muscle monitoring is described. The validation process was carried out on healthy subjects performing a voluntary contraction, in order to analyze the behavior of the system in a standard fatigue assessment setup as testified in literature [58], [33], [60], [61].

4.1 Voluntary Contraction Fatigue Recording

The validation of the system was conducted on 14 volunteers, 7 males and 7 women (age 24-31 years old, height 170.64±11.27, weight 66.5±11.66). The main purpose of this validation process was to compare the MMG fatigue parameters trends obtained from both the analog and the digital microphones with the trends obtained from EMG signal, widely used in literature for muscle fatigue analysis [31]. When studying muscle fatigue, the typical setup is an isometric voluntary contraction performed maintaining a constant force [58] [33] [60] [61], that does not involve movement artifacts or a distance changes between the muscle fibers and the recording sensors. In order to define a protocol, it is necessary to set a duration of the fatiguing exercise, that can be fixed [62] or subject-dependent, hence it is interrupted when exhaustion occurs [33]. In addition, a further validation protocol can be provided by recording the signal before and after the fatiguing exercise and comparing the two [58].

In this work, two validation protocols (figure 4.1) were established, both involving the *biceps brachii* muscles. The validaton protocols are described as follows:

- Two minutes without added weight, three minutes supporting a 3 kg weight fixed at the wrist, two minutes without added weight.
- Two minutes without added weight, supporting a 3 kg weight fixed at the wrist until exhaustion, two minutes without added weight.

(a)

(b)

Figure 4.1: **Validation protocols.** a: two minutes without added weight, three minutes supporting a 3 kg weight fixed at the wrist, two minutes without added weight. b: two minutes without added weight, supporting a 3 kg weigth fixed at the wrist until exhaustion, two minutes without added weight.

All contractions were isometric, with an angle between arm and forearm equal to 90°. In the second protocol, the exhaustion was identified as the moment in which this angle increased by 5°, as the change of angle is an actual indication of fatigue [31]. A professional goniometer by *Schupp* was used to evaluate the angle variations, with a 30 cm ruler placed on the subject open hand as a reference.

The EMG signal was acquired by means of three pre-gelled electrodes (Covidien, 24 mm ⊘, interelectrode distance 25 mm), two placed at the belly of the biceps muscle, one places at the elbow as reference.The electrodes were placed by following the *Surface ElectroMyoGraphy for the Non-Invasive Assessment of Muscles* (SENIAM) standard recommendation. The design of the 3D printed microphones plastic cases allowed to sew them to an adjustable bracelet, as previously shown in figure 3.7. In this way, MMG sensors (digital and analog microphones) were placed athwart the orientation of EMG electrodes, on the muscle belly. Sensor location is particularly important for the repeatability and reliability of EMG signal, while for MMG sensors is less crucial [37]. This is one of the main advantage of MMG technique in muscle fatigue estimation.

4.2 Results

This section displays the results obtained from the experimental validation of the system. In order to show effectively the results obtained by the two protocols, the fatigue parameters obtained by all the subjects were averaged and plotted with respect to the percent contraction time. For the second protocol, considering that contraction time was different for each volunteer, 26 points were averaged in order to obtain the parameters trend for every 4% of the contraction time. In addition, a linear regression was computed for every parameter trend [60], by means of MATLAB® *polyfit* and *polyval* functions. The approach used was the least squares best fit. The coefficient of determination R^2 was also assessed for each regression using equation 4.1. In this equation y represents the averaged data, $\bar{y}$ is the mean of y and Y are the calculated values of y.

$$R^2 = 1 - \frac{\sum_{i=1}^{n}(y_i - Y_i)^2}{\sum_{i=1}^{n}(y_i - \bar{y}_i)^2} \tag{4.1}$$

The resulting fatigue plots are shown in figures 4.2, 4.3, 4.4, 4.5, 4.6 and 4.7. Each observation present the standard error (SE) bar, computed as showed in equation 4.2. In this equation, σ is the data standard deviation, and n is the number of observations.

$$SE = \frac{\sigma}{\sqrt{n}} \tag{4.2}$$

It has been reported in literature [14][60] that amplitude parameters, such as Average Rectified Value (ARV) and Root Mean Square (RMS), should increase during a fatiguing contraction of the isometric, constant force type defined in this work protocols. Frequency parameters, on the contrary, have shown a decreasing trend in previous studies [14][60]. The first protocol results does not reflect this trends completely. As regards the EMG signal, amplitude parameters ARV and RMS both decrease in time. In fact, observing figures 4.2, 4.3 and 4.4 the linear regressions of these parameters present a negative linear coefficient, making the trend to decrease in time. Furthermore, the MMG signal recorded by the digital microphone shows an increase of the Mean Frequency (MF) parameter, not following the expected trend.

The second protocol showed more promising results. Parameters trend is the one expected for each sensor, proving that a protocol that involves an exhaustion assessment is more reliable because it takes into account the different endurance of each subject. Observing linear regressions for each amplitude parameter in figure 4.5, 4.6 and 4.7, the trend is always increasing in time. On the other hand, the MF parameter presents an evident drop in time for each sensor, as expected from literature trends. It is interesting to consider that an higher variability for EMG is evident, while for MMG, regardless of the type of microphone, standard error is visibly lower. This is probably due to the sensors location; as already pointed out, EMG electrodes location is more crucial than the one of the microphones [37]. This result seem to indicate that MMG signal recorded by MEMS condenser microphones is more reliable than EMG signal.

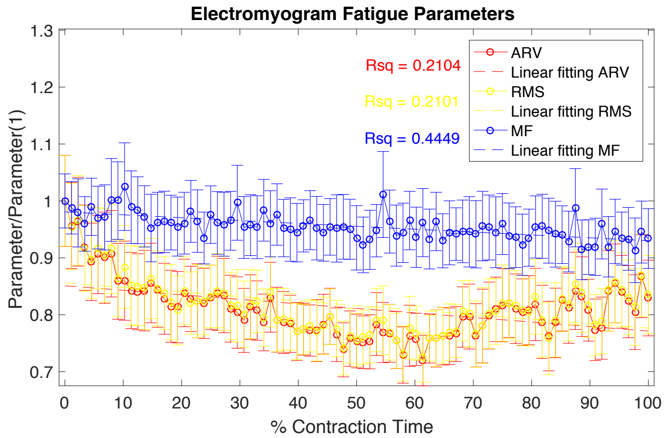

Figure 4.2: **Electromyogram fatigue parameters trends for the first protocol.** All values are normalized to the first one. Linear regression is shown for each parameter trend, along with the coefficient of determination R^2.

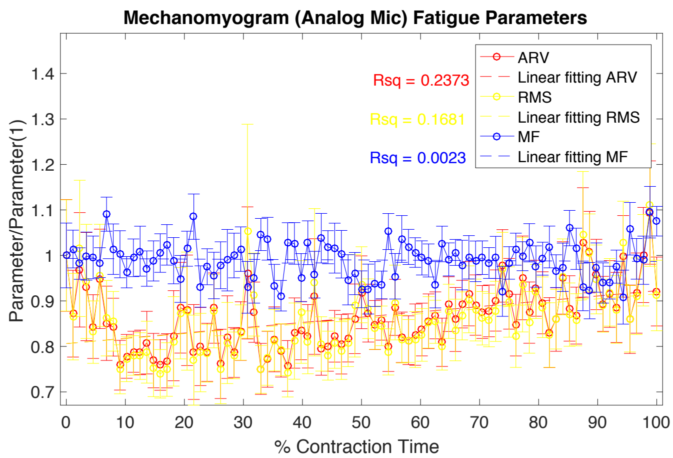

Figure 4.3: **Mechanomyogram from analog microphone fatigue parameters trends for the first protocol.** All values are normalized to the first one. Linear regression is shown for each parameter trend, along with the coefficient of determination R^2.

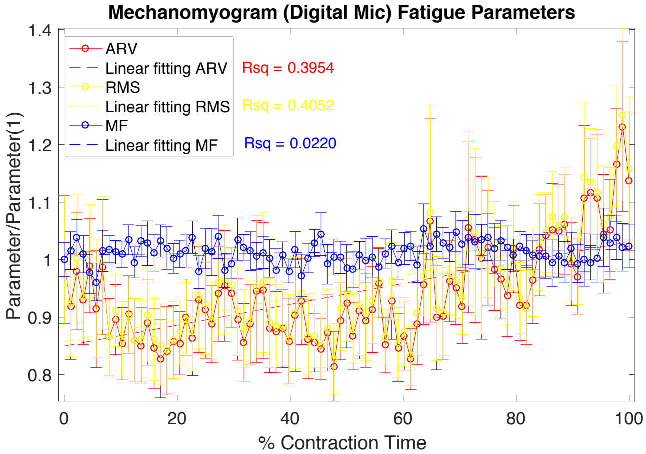

Figure 4.4: **Mechanomyogram from digital microphone fatigue parameters trends for first protocol.** All values are normalized to the first one. Linear regression is shown for each parameter trend, along with the coefficient of determination R^2.

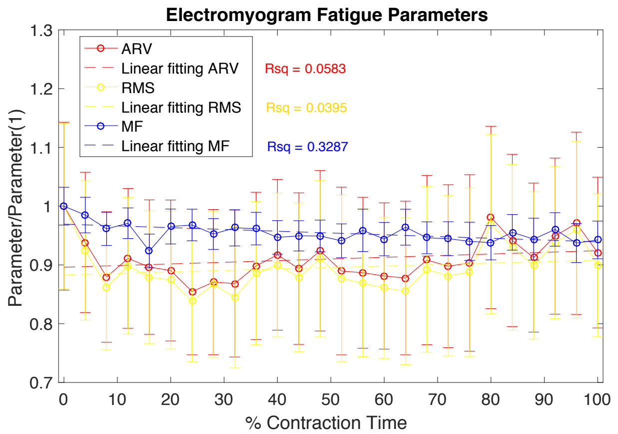

Figure 4.5: **Electromyogram fatigue parameters trends for the second protocol.** All values are normalized to the first one. Linear regression is shown for each parameter trend, along with the coefficient of determination R^2.

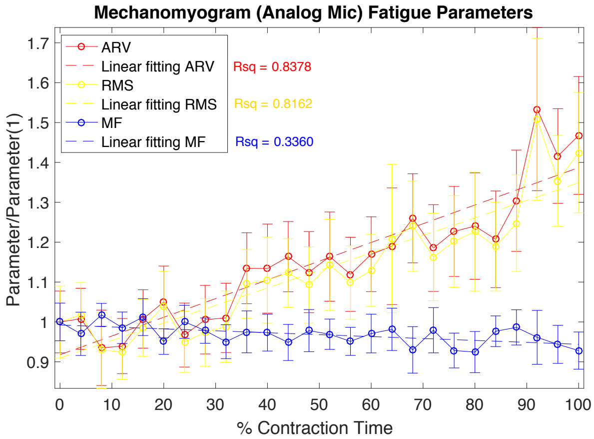

Figure 4.6: **Mechanomyogram from analog microphone fatigue parameters trends for the second protocol.** All values are normalized to the first one. Linear regression is shown for each parameter trend, along with the coefficient of determination R^2.

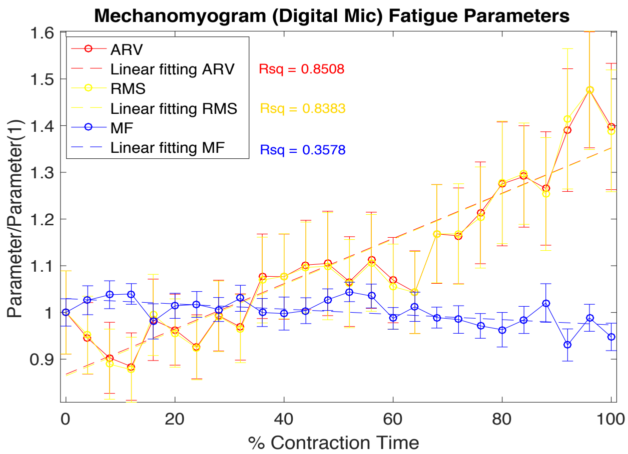

Figure 4.7: **Mechanomyogram from digital microphone fatigue parameters trends for the second protocol.** All values are normalized to the first one. Linear regression is shown for each parameter trend, along with the coefficient of determination R^2.

The electromyography signal amplitude parameters present, as already stated, a relevant variability with respect to the microphones trends. Moreover, the linear regression slope appear to be visibly lower. In fact, the EMG regression line presents a 5% increase with respect to the first value, while for both microphones the increase is about the 50%, as showed in figures 4.5, 4.6 and 4.7. The correlation between averaged sensors parameters is displayed in figures 4.8, 4.9 and 4.10 along with the correlation coefficient. Its value was obtained by means of equation 4.3, computed by the MATLAB® function *corr2*.

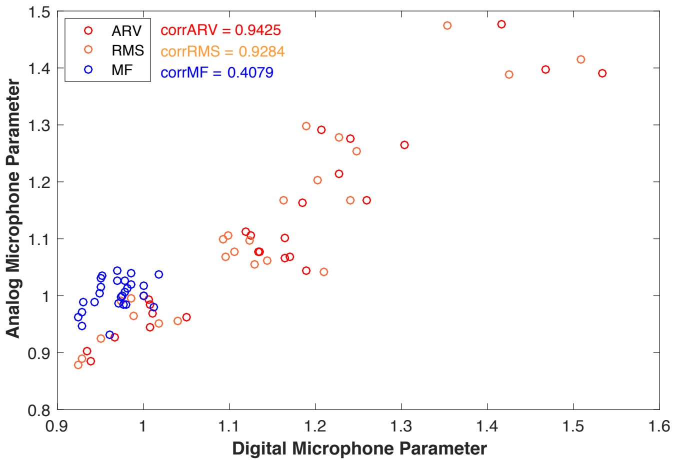

Figure 4.8: **Correlation between analog microphone parameters and digital microphone parameters.**

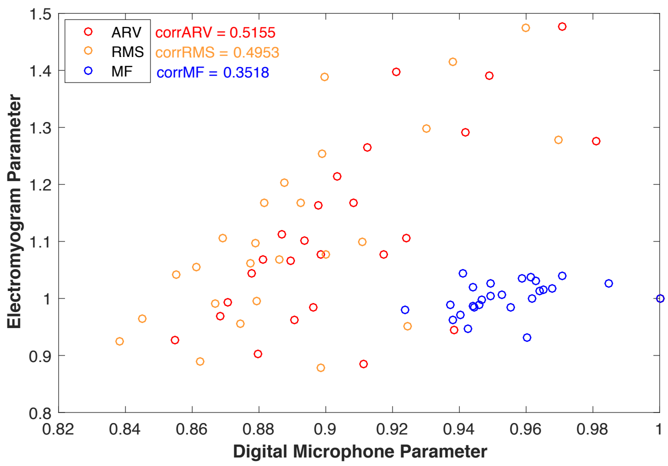

Figure 4.9: **Correlation between electromyography parameters and digital microphone parameters.**

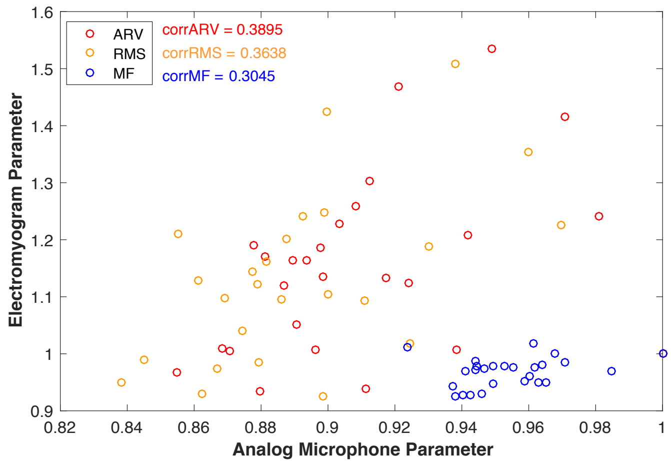

Figure 4.10: **Correlation between electromyography parameters and analog microphone parameters.**

A high correlation is present between the two microphones amplitude parameters ($corrARV = 0.94$, $corrRMS = 0.92$). The digital microphone is able to provide reliable results, if compared to the analog microphone. On the other hand, electromyography amplitude variation is poorly correlated to the one of mechanomyogram (digital microphone: $corrARV = 0.51$, analog microphone: $corrARV = 0.38$), proving the robustness of the microphones with respect to sensors location.

$$corr = \frac{\sum_n (x_n - \bar{x})(y_n - \bar{y})}{\sqrt{(\sum_n (x_n - \bar{x})^2)(\sum_n (y_n - \bar{y})^2)}} \tag{4.3}$$

Statistics histograms computed for the second protocol, showing the linear coefficient (slope) from each parameter regression, are showed in figures 4.12, 4.13 and 4.14. They were obtained by means of the *histogram* MATLAB function, able to estimate the suitable number of bins in order to show the data distribution shape. Among the 14 subjects, 7 showed a decreasing fitted trend for the amplitude parameters. An example of a fatigue plot that does not present expected trend is shown in figures 4.11a, 4.11b and 4.11c. As regards the microphones results, on the contrary, their amplitude slopes mostly belong in the positive range. Besides, their values distribution is analogue.

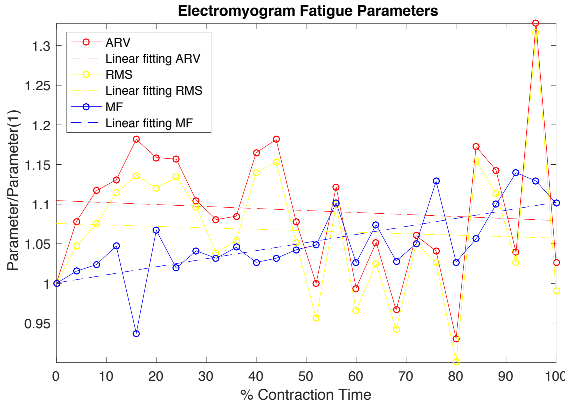

(a)

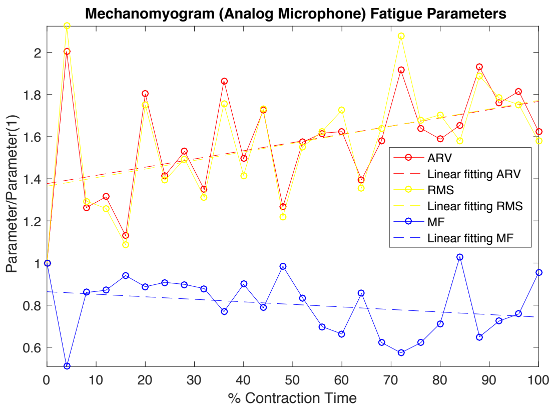

(b)

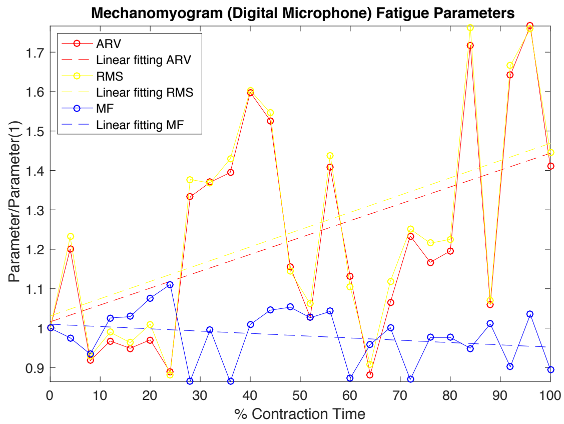

(c)

Figure 4.11: **Example of one non-compliant subject parameters trends** a: electromyogram fatigue parameters trends. b: mechanomyogram from analog microphone fatigue parameters trends. c: mechanomyogram from digital microphone fatigue parameters trends. All values are normalized to the first one. The EMG parameters trends are not the ones expected in literature.

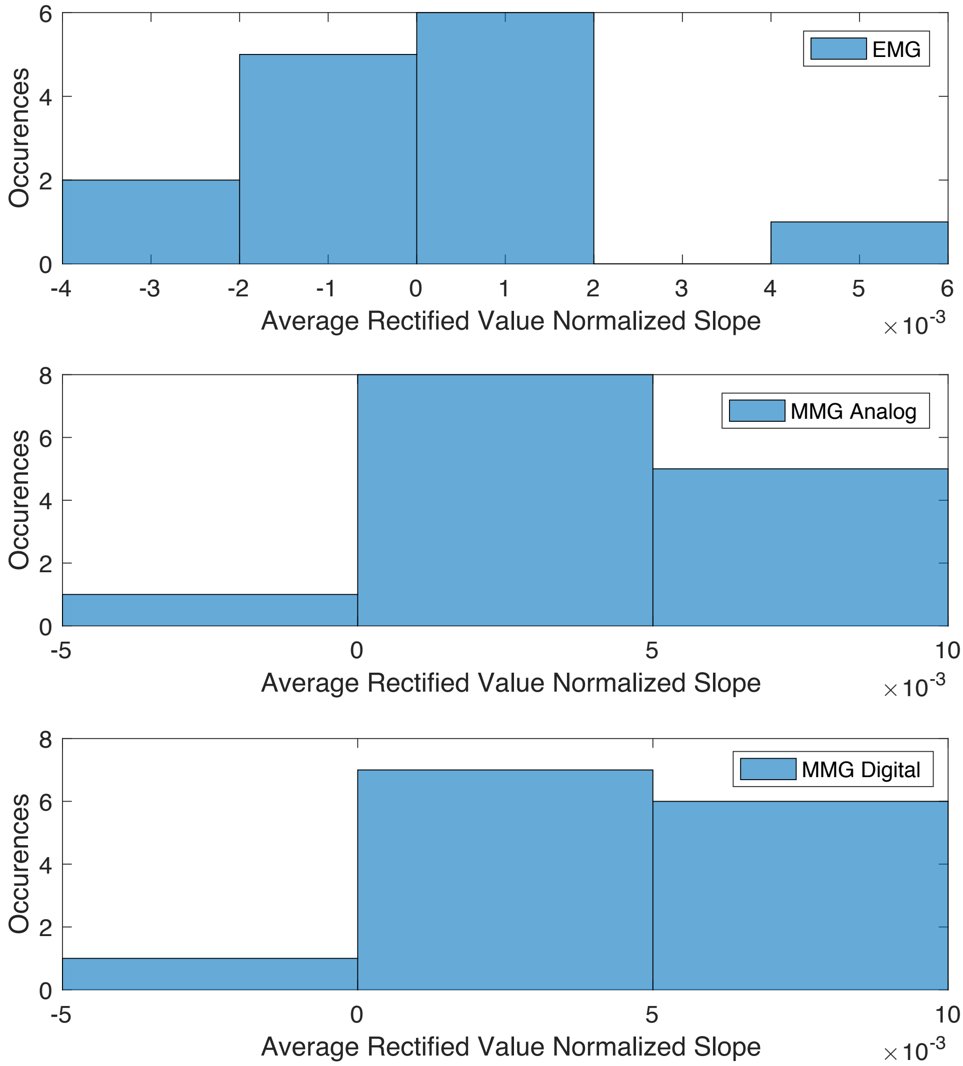

Figure 4.12: **Average Rectified Value slope histogram for the second protocol.** Values were normalized to the first one when computing the slope.

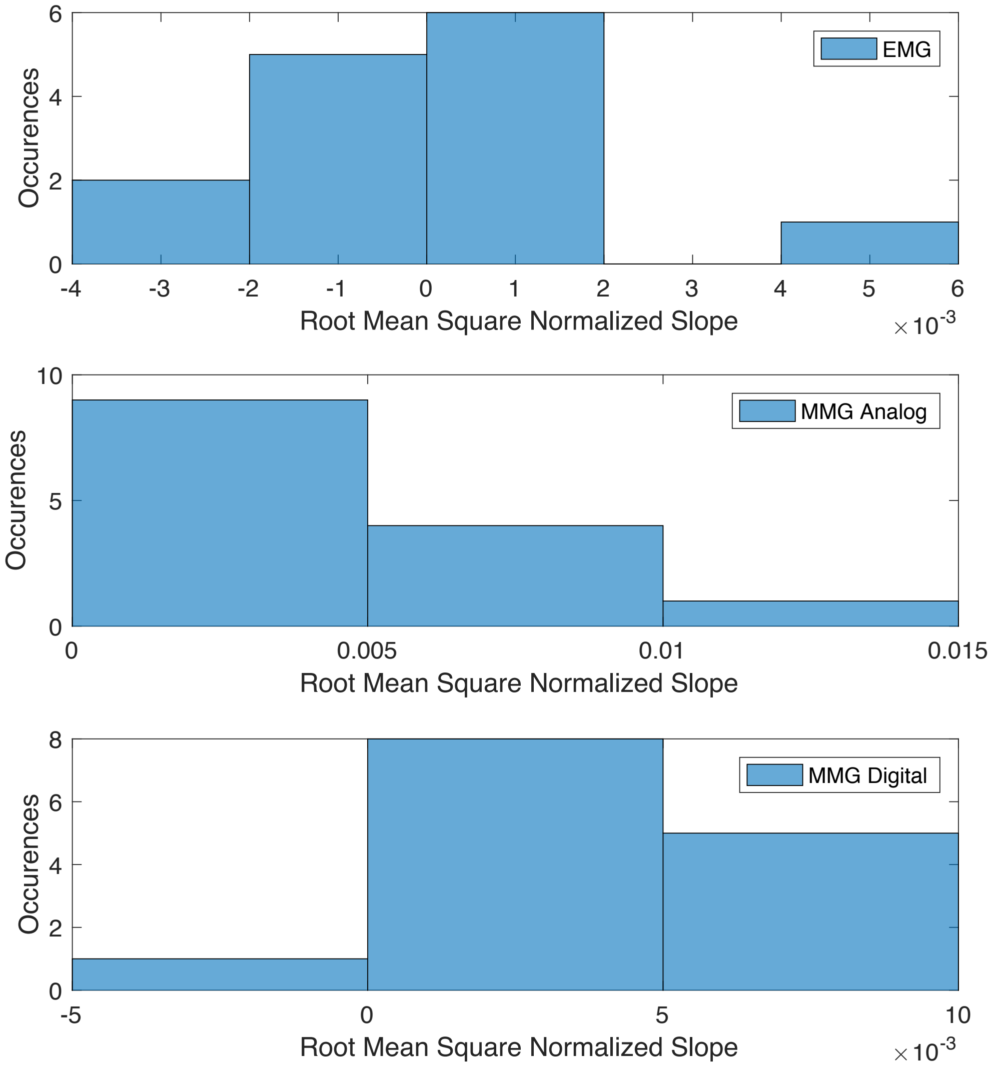

Figure 4.13: **Root Mean Square slope histogram for the second protocol.** Values were normalized to the first one when computing the slope.

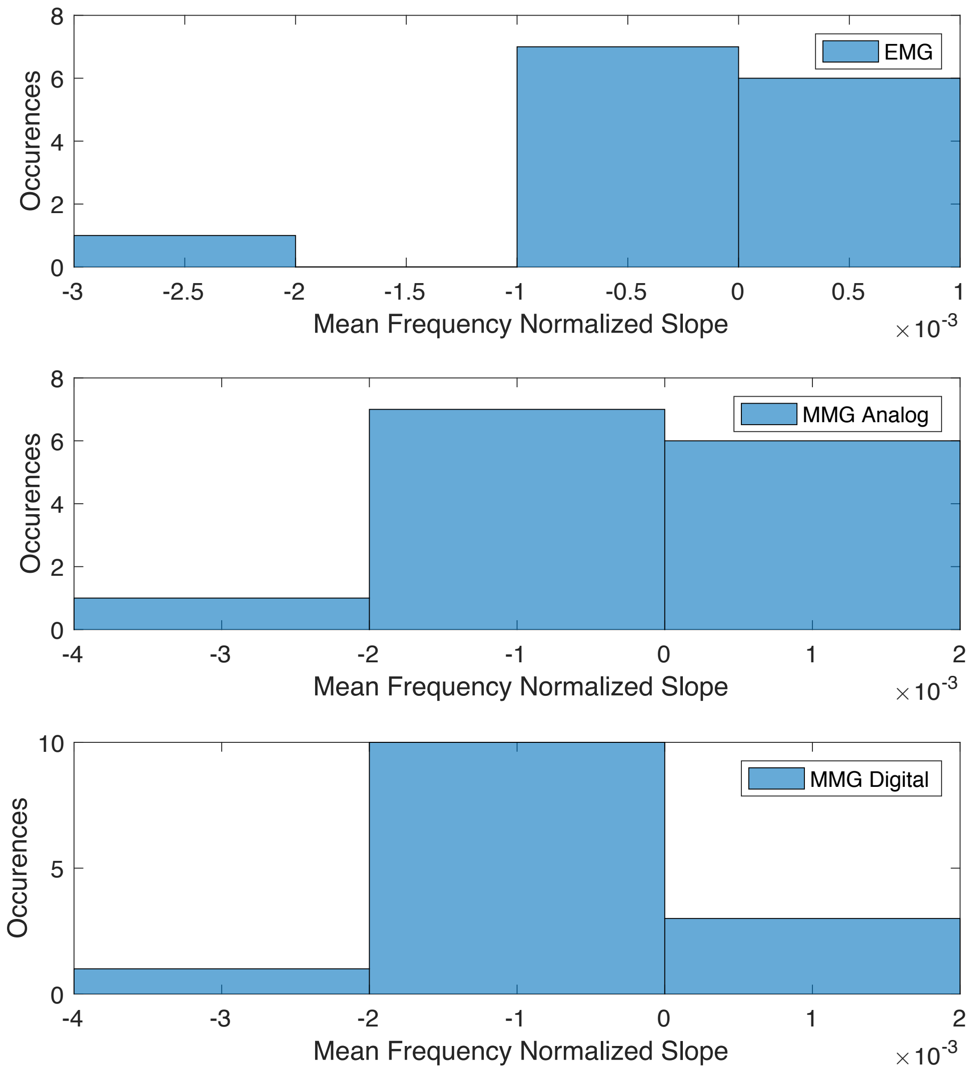

Figure 4.14: **Mean Frequency slope histogram for the second protocol.** Values were normalized to the first one when computing the slope.

Since the digital microphone integrated on SensorTile module is not designed for low frequency signals recording, we wanted to validate and prove its performance in signal acquisition below 100 Hz. Therefore, we conducted the experiments by adding a second SensorTile module identical to the one on the skin of the subject as control, that was placed on the table in front of the subject to acquire the room background noise. The main purpose was to prove that the signal recorded by the SensorTile on the subject is different from the background noise, thus that it derives from the muscle activity. In figure 4.15 the PSDs of the two signals are shown, normalized to the maximum value of the MMG recording SensorTile. It is evident how the two frequency spectra are different, proving the reliability of the digital microphone as MMG sensor.

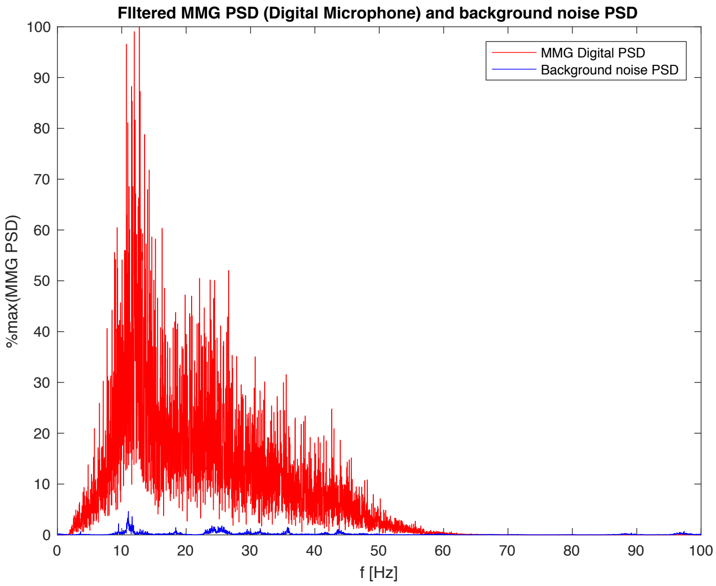

Figure 4.15: **PSD comparison.** Digital microphone mechanomyography signal PSD in comparison with background noise PSD. The recording was carried out by two identical SensorTile modules.

By considering the recordings acquired before and after the fatiguing exercise, results are shown in figures 4.16, 4.17, 4.18 for the first protocol, and in figures 4.19, 4.20 and 4.21 for the second protocol. In agreement with the literature [14], an increase of amplitude parameters and a decrease of frequency parameters should be assessed comparing trends before and after fatigue. In the first protocol, results are not consistent with expected trends: EMG amplitude parameters tend to decrease, while MMG frequency parameters tend to increase. The second protocol shows more reliable results, as ARV and RMS undergo a clear increase, even if MF does not show an effective drop; it rather tend to grow, in particular in the signal acquired with the digital microphone. Probably this inconsistency is due to the recovery time between the fatiguing exercise and the following recording, that was in average 10 minutes.

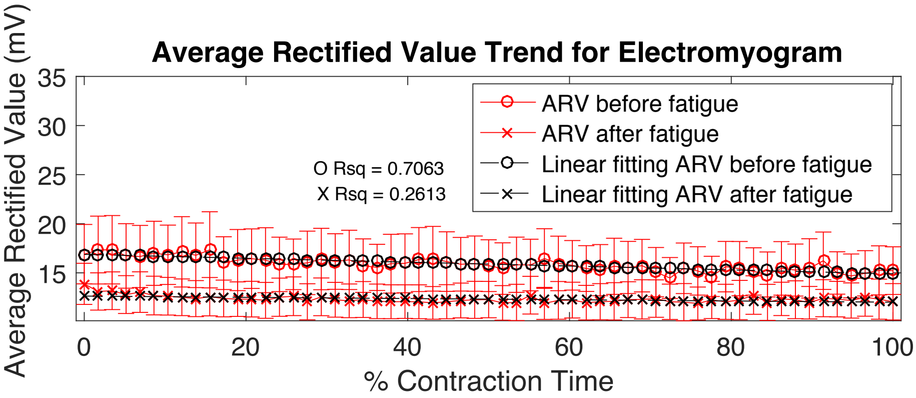

(a)

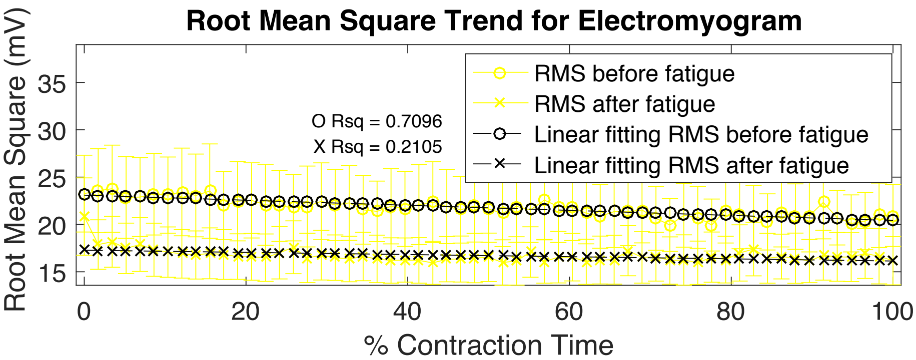

(b)

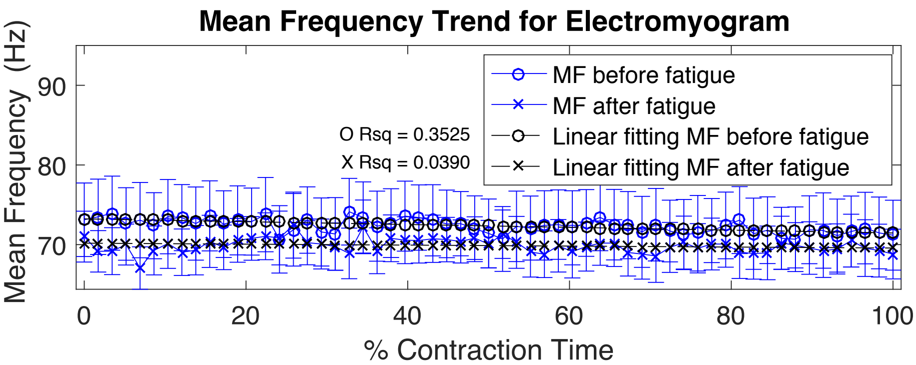

(c)

Figure 4.16: **First protocol pre and post fatigue results for the electromyogram** a: ARV trends. b: RMS trends. c: MF trends.

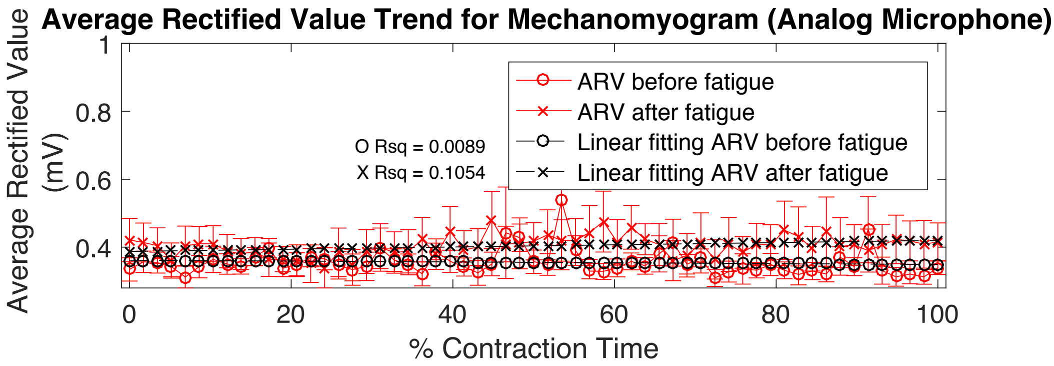

(a)

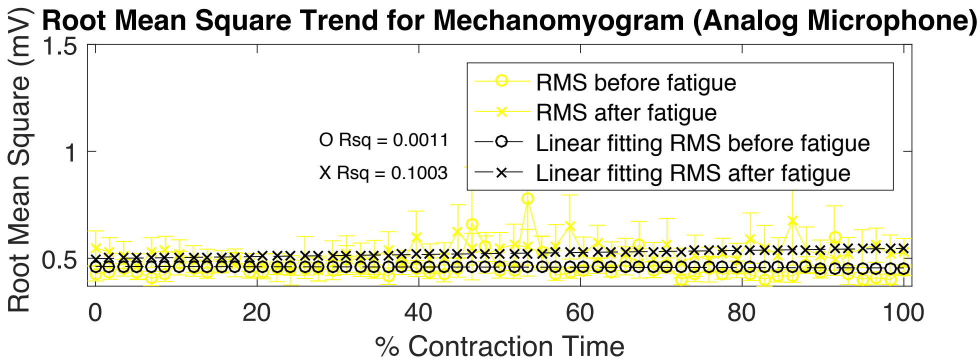

(b)

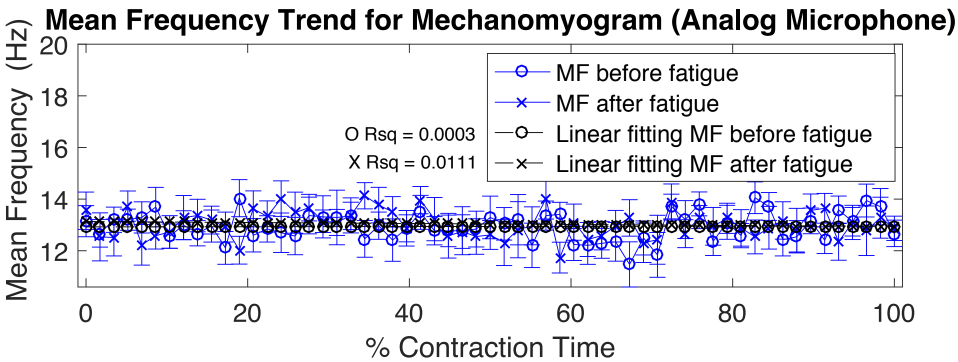

(c)

Figure 4.17: **First protocol pre and post fatigue results for the mechanomyogram (analog microphone).** a: ARV trends. b: RMS trends. c: MF trends.

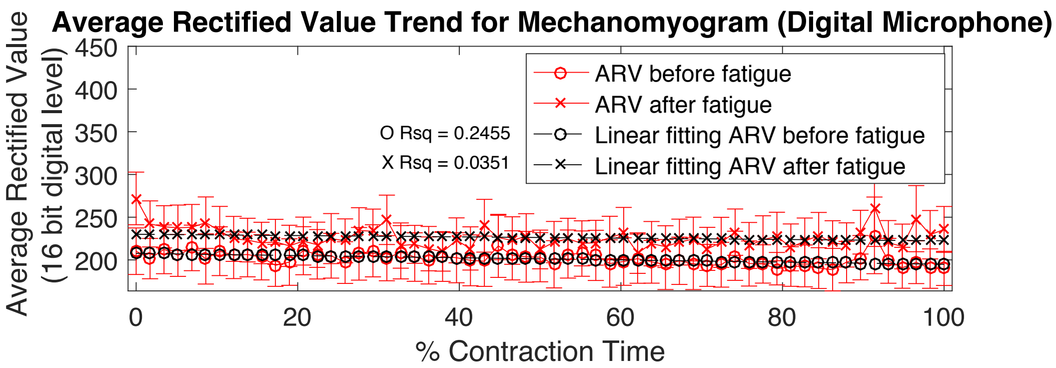

(a)

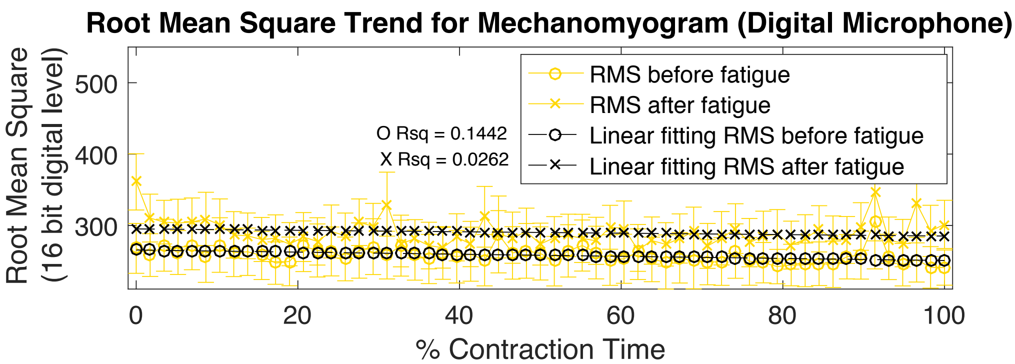

(b)

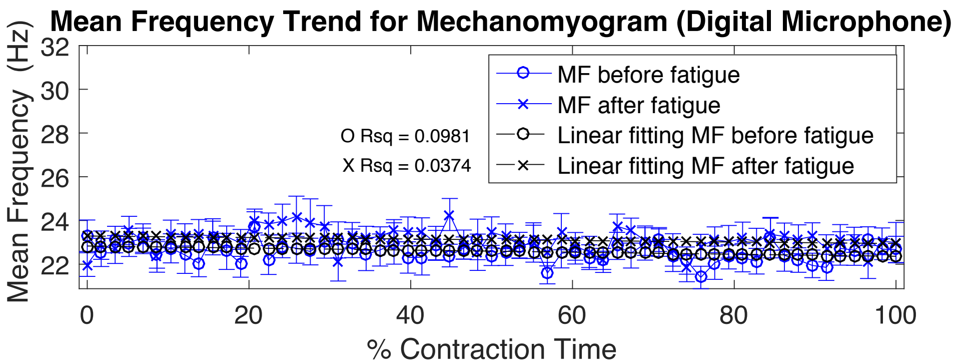

(c)

Figure 4.18: **First protocol pre and post fatigue results for the mechanomyogram (digital microphone).** a: ARV trends. b: RMS trends. c: MF trends.

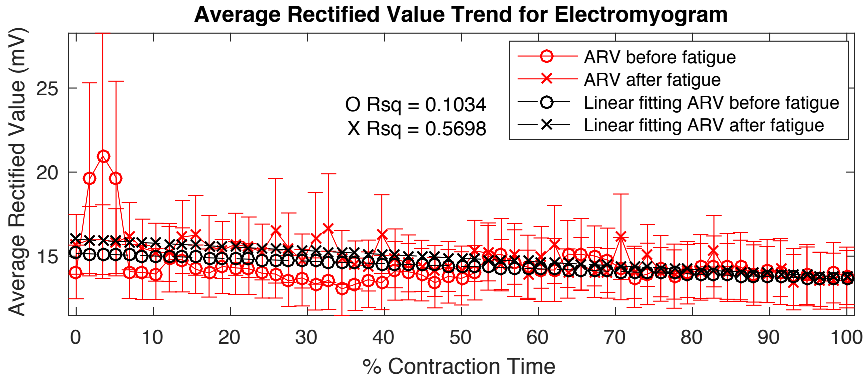

(a)

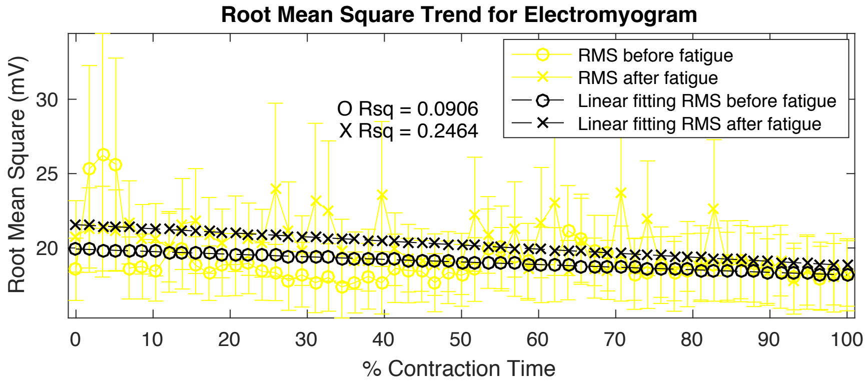

(b)

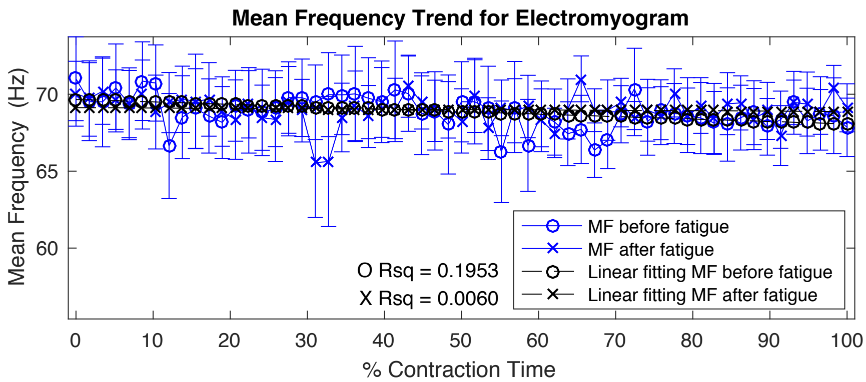

(c)

Figure 4.19: **Second protocol pre and post fatigue results for the electromyogram** a: ARV trends. b: RMS trends. c: MF trends.

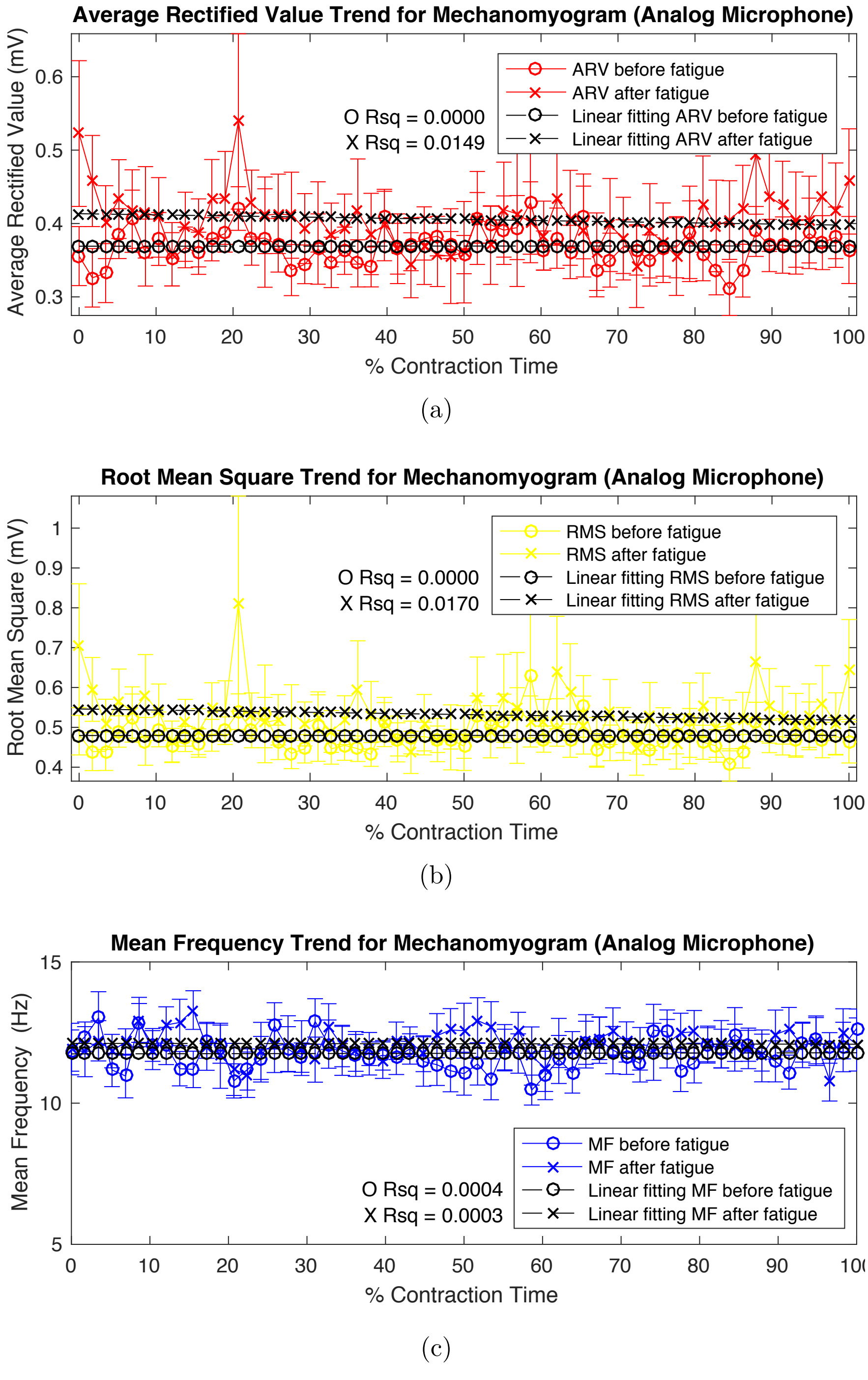

Figure 4.20: **Second protocol pre and post fatigue results for the mechanomyogram (analog microphone).** a: ARV trends. b: RMS trends. c: MF trends.

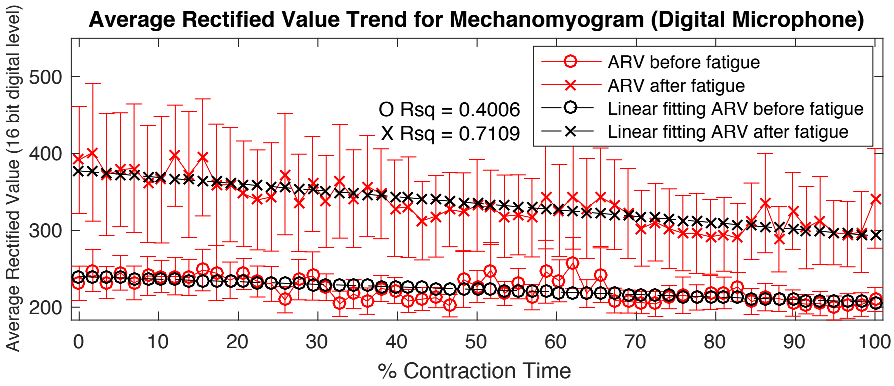

(a)

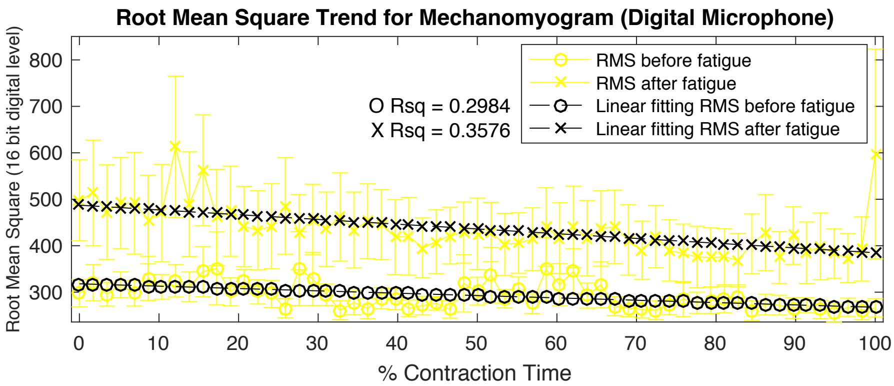

(b)

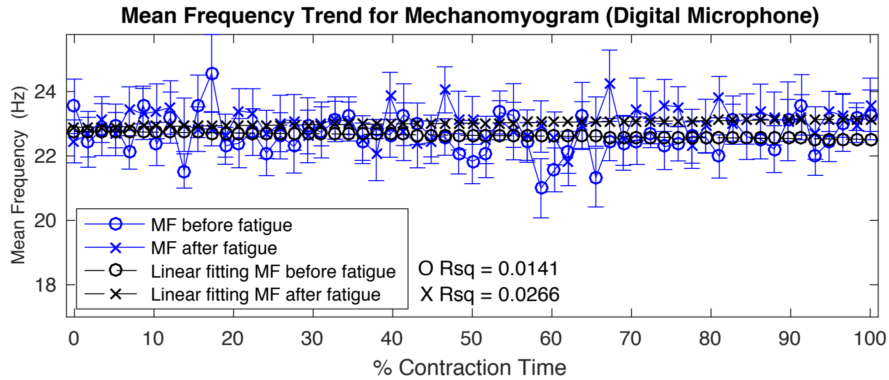

(c)

Figure 4.21: **Second protocol pre and post fatigue results for the mechanomyogram (digital microphone)** a: ARV trends. b: RMS trends. c: MF trends.

4.3 Discussion

The main purpose of this thesis work was to realize and validate a fatigue feedback system suitable for electrical stimulation rehabilitation techniques. The mechanomyography signal was selected because of its multiple advantages. Firstly, during an electrical stimulus, the MMG transducers are not affected by electrical artifacts, since the nature of the signal is utterly mechanical. This feature allows a simpler electronic design, without stimulus blanking strategies. Moreover, the mechanomyogram acquisition presents some advantages with respect to electromyography. The transducer placement result less relevant, not affecting as much the signal amplitude. This feature contributes to the easy usage of the MMG technique, along with the unnecessary skin surface preparation before each acquisition.

Mechanomyography signal can be sensed at the skin surface by means of different transducers. Condenser microphones were selected for their robustness to motion artifact, considering the dynamic movements usually induced by functional electrical stimulation techniques. In particular, MEMS technology was considered because of the high integration and small dimensions, useful features when it comes to wearable rehabilitation systems. For this reason, the *ST Microelectronics* MEMS digital microphone integrated on *SensorTile* module was finally picked for the system design. This particular acoustic transducer is designed for vocal applications, with no provided information about its behaviour at the MMG low-frequencies. In order to characterize the digital microphone, a second reference MMG transducer was taken into account during the validation of the system. In fact, well beyond to previous tests inside an anechoic chamber, it was necessary to compare the digital microphone results with the ones obtained from a previously validated condenser microphone.

The system validation was carried out in a standard configuration, using the electromyography signal recording as a reference for muscle fatigue assessment. The two proposed validation protocols returned different results. The first protocol, not considering the personal timing of muscle fatigue development of each subject, proved to be the less reliable. In fact, amplitude parameters for the EMG signal have not show the typical increasing trend. Both condenser microphones, on the contrary, seem to return the expected trends for what concerns amplitude parameters. The line increment for the analog microphone is about the 10% with respect to the initial value, while for the digital microphone it is almost the 20%. As regards the frequency parameter trend, the EMG mean frequency shows almost a 5% decrease, while both microphone does not seem to indicate a relevant drop for the frequency content. The digital microphone mean frequency rather tends to slightly grow. Overall, the parameters trends does not result adherent to the literature indications, thus no conclusion can be made about sensors performances for the first protocol.

On the ther hand, the second protocol, showed promising results. In fact, EMG and MMG parameters trends seem to be adherent to previous literature findings. This proves the higher efficiency of custom exercises, able to respect the personal timing of fatigue development. In particular, mean frequency showed a 5% decrease for the electromyogram and the mechanomyogram recorded by both microphones. Amplitude parameters, however, require a deeper discussion. The increase is evident for the three different sensors, being almost the 50% of the initial value for the MMG signals acquired for both microphones, and only the 5% in the case of the electromyography signal. This important difference is due to the fact that the exact half of the subjects (7 over 14) showed a negative linear coefficient for the amplitude parameters linear regression. Moreover, the standard error for electromyogram is visibly higher when compared to the mechanomyogram variability of both microphones. This result seem to indicate that MMG is less affected by the differences in transducer location and noise inter-subjects. The EMG amplitude, in fact, is known to be highly influenced by electrodes placement over the muscle fibers. Condenser microphone, on the other hand, proved a significant robustness.

The digital microphone results are highly comparable to the analog microphone ones, demonstrating its suitability for MMG recording and muscle fatigue assessment applications. In fact, the amplitude parameters slope was significantly correlated to the analog microphone ($corrARV = 0.94$, $corrRMS = 0.92$), presenting the highest correlation between mean frequency slopes ($corrMF = 0.41$). A further reliability test is represented by the second *SensorTile* module included for background noise recording, showing a significantly different frequency spectrum with respect to the signal recorded on the subject's skin. The *SensorTile* digital microphone can then be used for muscle fatigue estimation during isometric fatiguing contractions, returning reliable results. The advantages of this system are various, including the easy-to-use smartphone application, the SD card data storage and the ensemble of the data provided by the other sensors integrated on the module, such as the accelerometer and gyroscope. After and post fatigue amplitude and frequency parameters computations are proving again that the first protocol is not adherent to expected trends. In fact, EMG amplitude parameters showed a significant drop of the linear regression, while the digital microphone mean frequency trend present an increase. The second protocol demostrated again the literature adherence with regards to amplitude parameters, but mean frequency parameters did not show a relevant change, a part for a slight increase of the microphones trends. This is probably due to the fact that the time period between the fatiguing contraction and the post fatigue recording was not assessed and standardized, being sometimes very different between subjects.

Chapter 5

Conclusions and Future Works

The fatigue estimation feedback is considered a fundamental integration for FES-based rehabilitation systems. Traditionally, elctromyography (EMG) signal is considered able to assess muscle fatigue. However, it is affected by electrical stimulation and dynamic movements artifacts, as well as by skin conductance changes. To overcome these limitations, the mechanomyography (MMG) signal resulted to offer a valid alternative to EMG. In fact, it is the mechanical expression of the muscle activity, so it is not affected by electrical stimulation or by skin conductance, not needing a speficific skin preparation.

Muscle fatigue systems comparison

Muscle fatigue feedback system	Muscle fatigue detection	Stimulation artifact robustness	Dynamic movement artifacts robustness	No skin preparation	Motion analysis sensors
Surface Electromyography Recording System	✓	✗	✗	✗	✗
Analog Condenser Microphone for Mechanomyography recording	✓	✓	✓	✓	✗
***SensorTile* for Mechanomyography Recording**	✓	✓	✓	✓	✓

Table 5.1: **Comparison among the muscle fatigue systems considered in this thesis.**

Furthermore, considering condenser microphones as MMG transducers, the motion artifact is minimized. In this thesis, two MMG-based muscle fatigue feedback systems were compared, one realised with a MEMS digital microphone inegrated on a commercial wearable module, the other with a MEMS analog microphone designed for low frequencies applications, such as mechanomyogram recording. In parallel, the mechanomyography signal fatigue parameters of both microphones were compared to the electromyogram parameters. The main characteristics of the muscle fatigue monitoring systems considered in this thesis works are summerized in table 5.1. The experimental validation of the system demostrated the suitability of the digital transducer for mechanomyography recording and muscle fatigue assessment, as its performances were comparable to the analog microphone ones. The wearable commercial module where the digital microphone is integrated presents also motion analysis sensors (e.g. accelerometer). For this reason, and considering its suitability for muscle fatigue monitoring, the module would be a useful tool in a complete rehabilitation system. Moreover, the mechanomyography signal recorded by the digital microphone proved its robustness to sensor location with respect to the electromyography signal, presenting a lower variability and more relevant fatigue parameters changes during the development of muscle fatigue.

The proposed MMG-based system confirmed the suitability of MMG signal for muscle fatigue monitoring, proposing a valid wearable commercial module for rehabilitation. Further insight would be achieved with different possible future works, listed below.

- **Electrical stimulation trials**. The condenser microphone transducer was selected for its suitability during dynamic electrical elicited contractions. In order to validate the system for rehabilitation, muscle fatigue parameters should be assessed during electrically stimulated muscle contractions. Trials should be effected on healthy and injured patients, in order to compare parameters trends. A validation for dynamic stimulated movements is fundamental for a future application of the proposed system, because functional electrical stimulation involves tasks as grasping, cycling and walking. The wearability of the proposed mechanomyography recording system makes it suitable for this application, providing Bluetooth connectivity for recording management and local data storage.

- **Time-frequency signal processing for dynamic movements**. The signal processing of the mechanomyography signal recorded during a dynamic contraction requires more recent and reliable processing techniques, such as time-frequency representation of the signal. In fact, the sudden changes of the signal frequency content cannot be detected by traditional power spectral density estimation. The analysis of the variation of the frequency spectrum in time can provide more reliable information, describing the fatigue development with a more significant interpretation.

- **Mechanomyography optimization**. The mechanomyographic signal does not require a precise transducer placement or a skin preparation. However, some factors are able to influence the signal. For the design of a rehabilitation system for muscle fatigue assessment, it is compulsory to take them into account. Considering that the mechanomyogram is the mechanical expression of the muscle activity, the pressure applied on the transducer during the recording represents a significant factor. In fact, if the transducer generates a high pressure on the skin, the muscular waves on the surface could be suppressed or modified. The estimation of the standard pressure to apply when attaching the MMG transducer to the skin could be an useful tool in order to obtain reliable and repeatable results. Another factor to consider is the optimization of the acoustic chamber for the specific microphone. In this thesis, both microphones were provided with the same acoustic conical chamber in order to compare their results. The acoustic chamber size and dimensions highly affects the output signal, because the skin vibration is transmitted to the microphone through the air inside of the chamber. A further analysis could be carried out, by assessing the chamber size and dimensions that yield the highest gain for the particular *ST Microelectronics* MEMS digital microphone.

5.1 Future Applications

The MMG-based muscle fatigue feedback proposed in this thesis was designed for functional electrical stimulation (FES), in particular during spinal cord injury rehabilitation. However, electrically elicited movements proved to be a useful exercise also for other applications. In this section, possible specific rehabilitation contexts where the proposed system could be applied are described and shown in figure 5.1.

- **EMG-based electrical stimulation**. The rehabilitation by means of FES systems can be applied with various approaches. In particular, the electrical stimulation can be triggered and driven by the muscular activity of a therapist, as described in the work of Rossi *et al.* [63]. In this case, the electromyography signal is acquired from the therapist muscle, then it is processed in order to recognize the muscle contraction. A professional stimulator, integrated on the system, is programmed with the suitable stimulation parameters. The electrical stimulus is then triggered whenever a muscle contraction is detected on the therapist, causing the respective contraction on the patient's muscle. This rehabilitation system could also be used in the case of emiplegic patients, acquiring the signal from the uncompromised limb, stimulating the other one. The fatigue feedback system proposed in this thesis can be integrated within a rehabilitation protocol such as the one described, in fact the BITalino Plugged

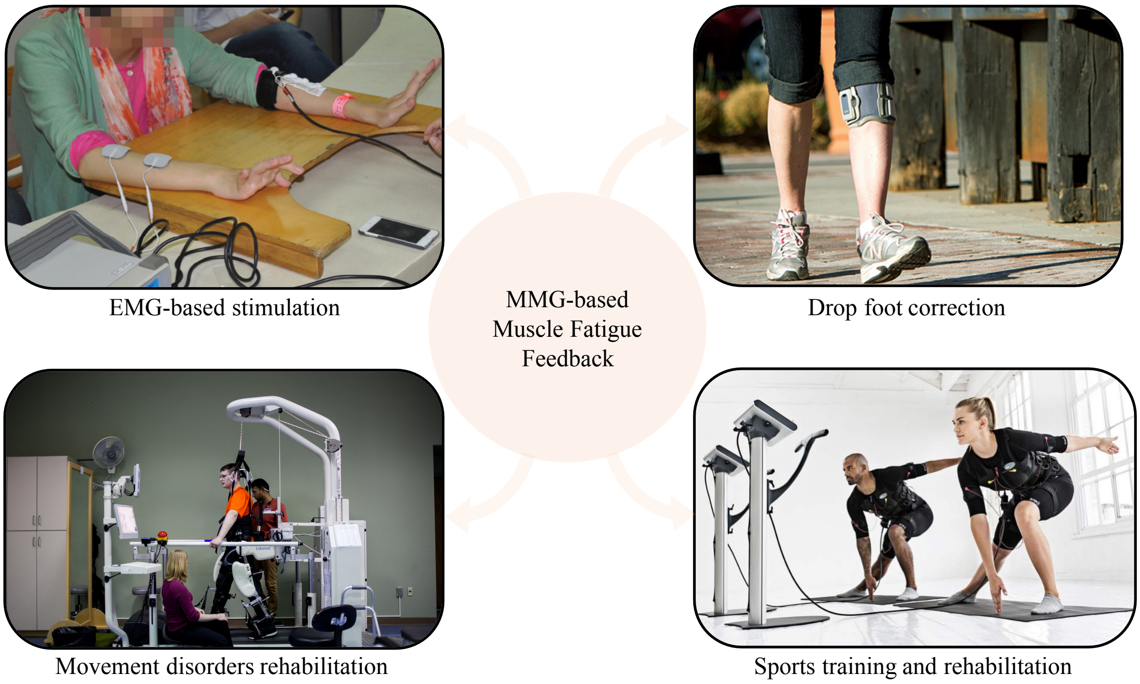

Figure 5.1: **MMG-based muscle fatigue feedback system applications**. EMG-based electrical stimulation (reprinted from [10]), movement disorders rehabilitation (reprinted from [11]), drop foot correction (reprinted from [12]) and sports training and rehabilitation (reprinted from [13]).

Board can be used for (i) the acquisition of the EMG signal, (ii) the acquisition of the MMG signal from the analog microphone and (iii) for triggering the stimulator. On the other hand, the wearable SensorTile module can provide not only the mechanomyography information, but also an interesting set of sensors considering the rehabilitation perspective of the system, as the accelerometer and the gyroscope.

- **Movements disorders rehabilitation**. Various medical conditions can lead to movements difficulties, such as multiple sclerosis and stroke. Functional electrical stimulation was proven to be effective for the improvement of upper limb function in multiple sclerosis patients [64]. Moreover, elicited contractions are often used to treating drop foot, a common condition in neuromuscular impaired subjects [65]. A muscle fatigue feedback as the one proposed in this thesis would support the rehabilitation, giving further information about the stimulated muscles.

- **Sports training and rehabilitation**. A combined approach of voluntary contractions and electrical stimulation can be used for sports training and rehabilitation [66]. For example, the electrical stimulation of the quadriceps muscle on soccer players after the anterior cruciate ligament reconstruction is able to improve the muscle strength [67]. The feedback system proposed would be able to monitor muscle fatigue during elicited and voluntary contractions, representing an useful tool for sports training and rehabilitation.

Chapter 6

Appendix

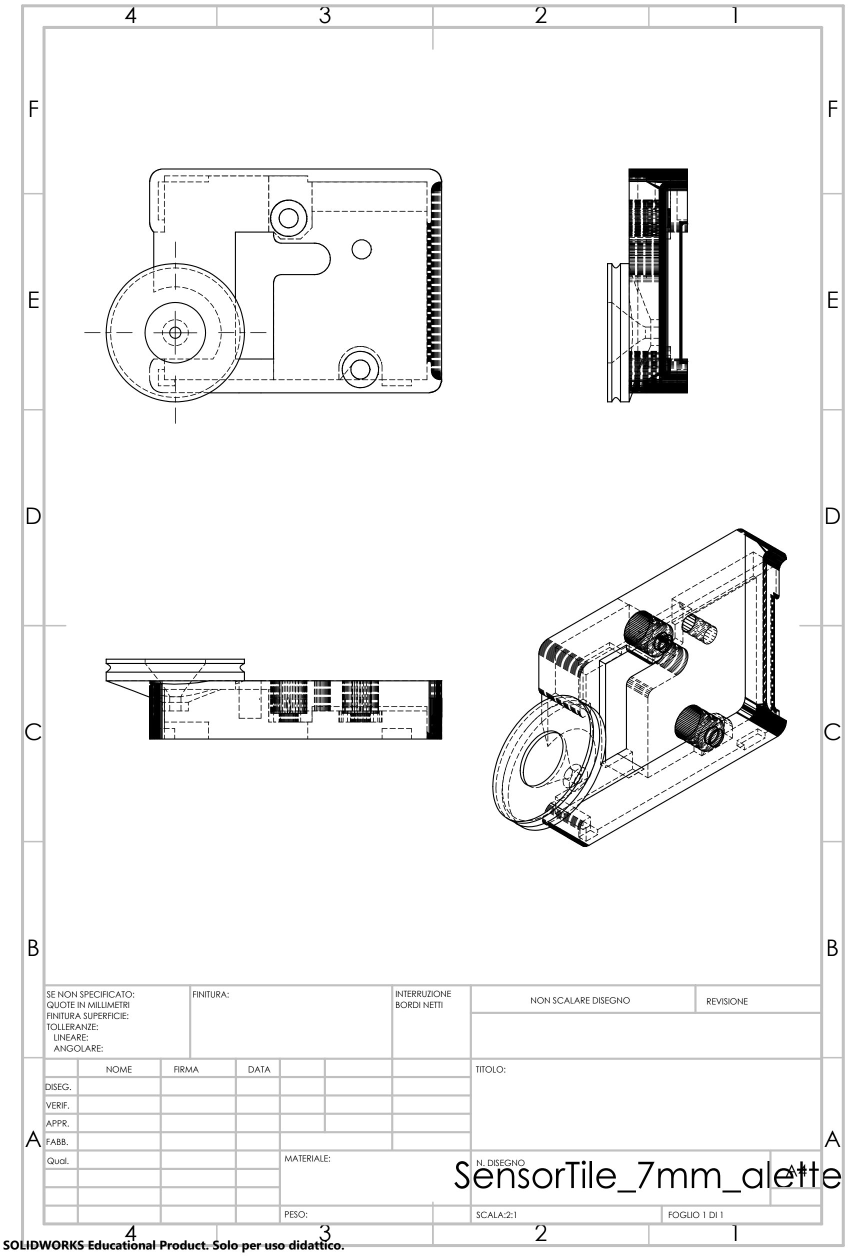

Figure 6.1: **SensorTile 3D printed acoustic chamber projections.**

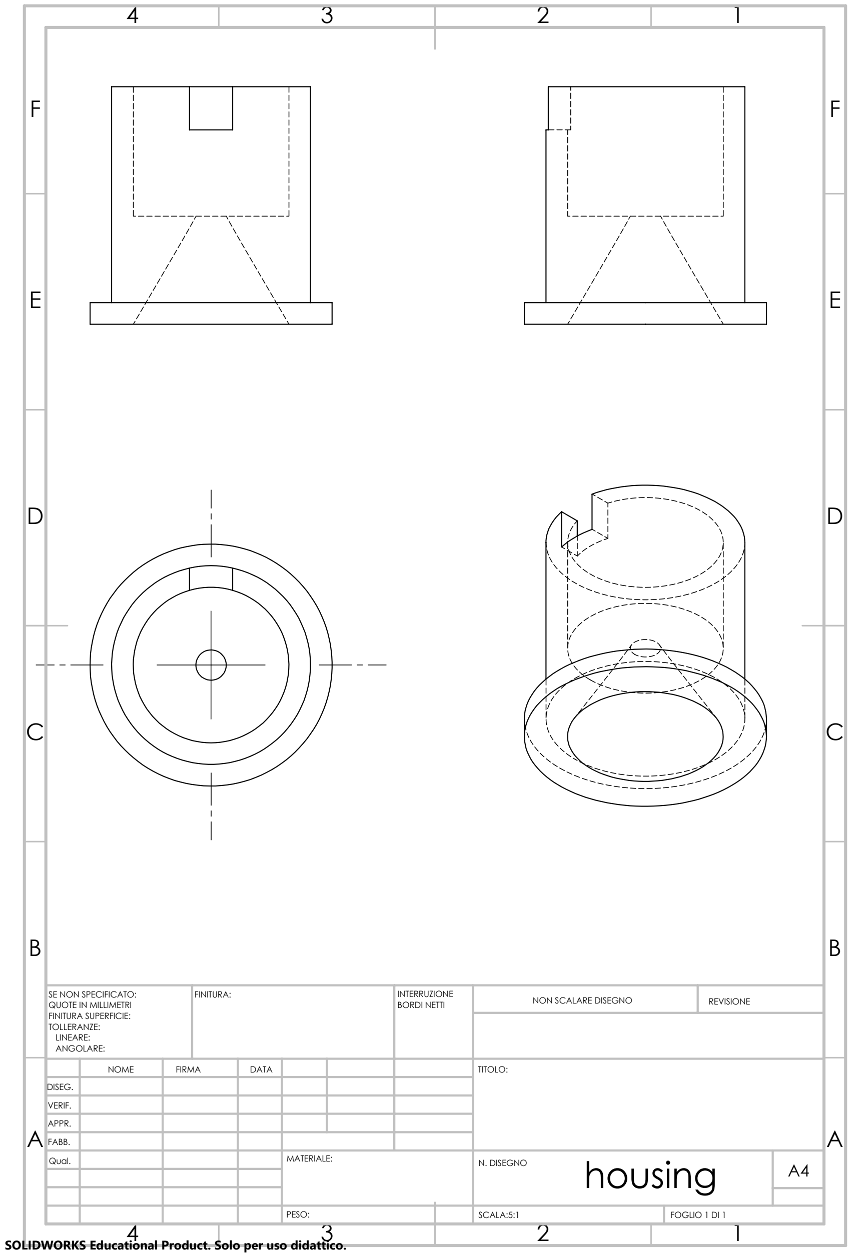

Figure 6.2: **Analog microphone 3D printed acoustic chamber projections.**

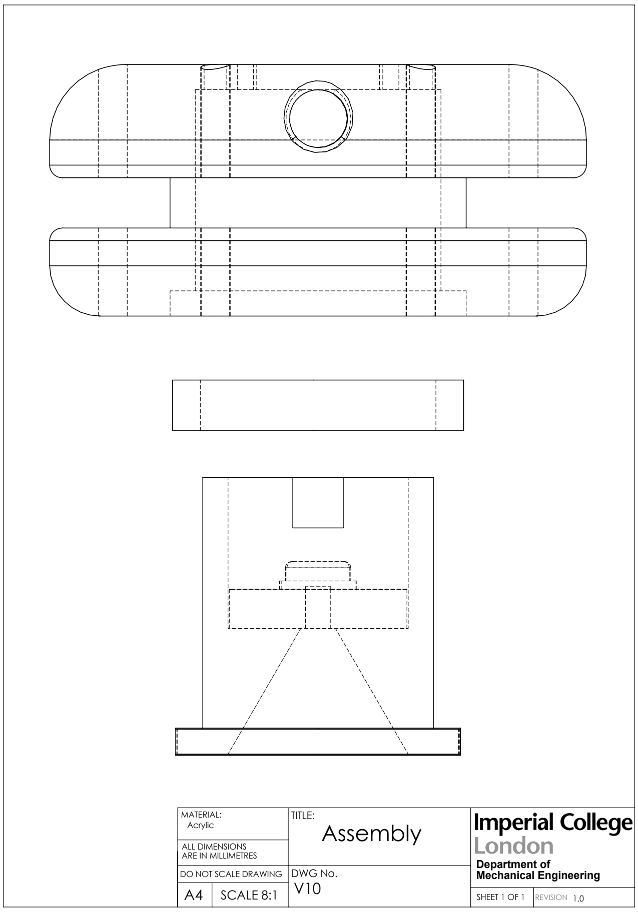

Figure 6.3: **Analog microphone 3D printed sensor case.** Reprinted from [14].

ThermoActive Software

PCB: Default Profiles
Component: Profile Lead free std

Profile Type: Auto Profile Mode

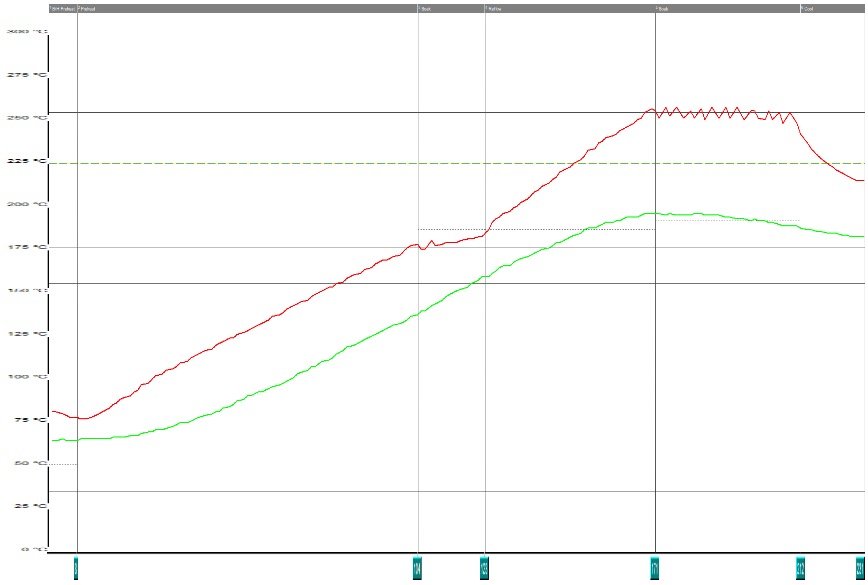

Max component temp: 248ºC. Max PCB temp: 189ºC. Liquidous temp: 217ºC, Time above liquidous: 69 seconds

Zone Title:	**B/H Preheat**	**Preheat**	**Soak**	**Reflow**	**Soak**	**Cool**
THPower (max):	0%	100%	20%	100%	80%	20%
TH Limit:	35ºC	170ºC	170ºC	245ºC	245ºC	150ºC
BH Power:	100%	80%	90%	95%	50%	0%
BH Limit:	50ºC	150ºC	180ºC	180ºC	185ºC	0ºC
Length:	5sec	136sec	2sec	38sec	25sec	14sec
Wait for PCB Temp	No	No	Yes	No	No	No
Ramp Rate:	0,00	1,00	0,00	2,00	0,00	-5,00
Cooling:	No	No	No	No	No	No

User:
Written By: Fred RENARD
Last Updated: 01/03/2018 by

06/03/2018 14:32:20

Figure 6.4: **Soldering Temperature Profile.**

Bibliography

[1] World Health Organization. International perspectives on spinal cord injury, 2013.

[2] C.L. Lynch and M.R. Popovic. Functional Electrical Stimulation. *IEEE Control Systems Magazine*, 28(2):40–50, 2008.

[3] B. Lindstrom, J. Lexell, B. Gerdle, and D. Downham. Skeletal Muscle Fatigue and Endurance in Young and Old Men and Women. *The journals of gerontology. Series A, Biological sciences and medical sciences.*, 52(1):B59–66, 1997.

[4] C. J. De Luca. *Muscles Alive*. Williams and Wilkins, 1985.

[5] STMicroelectronics. *AN4426 Application note - Tutorial for MEMS microphones*, 2014.

[6] Texas Instruments Bonnie Baker. *How delta-sigma ADCs work, Part 2*, 2011.

[7] Texas Instruments Bonnie Baker. *How delta-sigma ADCs work, Part 1*, 2016.

[8] STMicroelectronics. *Getting started with the STEVAL-STLKT01V1 SensorTile integrated development platform*.

[9] STMicroelectronics. *SensorTile development kit*.

[10] Z. Huang, Z. Wang, X. Lv, Y. Zhou, H. Wang, and S. Zong. A novel functional electrical stimulation-control system for restoring motor function of post-stroke hemiplegic patients. `http://www.nrronline.org/article.asp?issn=1673-5374;year=2014;volume=9;issue=23;spage=2102;epage=2110;aulast=Huang`.

[11] Omaha Media Group. A novel functional electrical stimulation-control system for restoring motor function of post-stroke hemiplegic patients. `https://www.madonnaomahacampus.org/technology-and-research/specialty-equipment`.

[12] Rachel Hosie. 20 minutes a week is supposedly all you need. `https://www.independent.co.uk/life-style/health-and-families/electrical-muscle-stimulation-what-is-it-how-work-20-minute-workout-lifesty` `html`.

[13] Quinn Phillips. Pros and cons of functional electrical stimulation for ms-related foot drop. `"https://www.everydayhealth.com/multiple-sclerosis/treatment/`

`pros-cons-functional-electrical-stimulation-ms-related-foot-drop/`.

[14] R. Woodward. *Pervasive Motion Tracking and Physiological Monitoring*. PhD thesis, The Imperial College of Science, Technology and Medicine Department of Mechanical Engineering, London, 2015.

[15] Federazione Associazioni Italiane Paratetraplegici. La lesione al midollo spinale. `http://www.faiponline.it/drupal/node/13`.

[16] M. Brodwin, W. Frances, J. Howard, and E. Brodwin, editors. *Medical, Psychosocial and Vocational Aspects of Disability*. Elliott and Fitzpatrick Inc, 2009.

[17] R. Nieuwenhuys, J. Voogd, and C. Van Huijzen. *Il sistema nervoso centrale*. Springer Science and Business Media, 2010.

[18] P. L. Jacobs and M. S. Nash. Exercise Recommendations for Individuals with Spinal Cord Injury. *Sports Med*, 34(11):727–751, 2004.

[19] K. Nas, L. Yazmalar, V. Şah, A. Aydın, and K. Öneş. Rehabilitation of spinal cord injuries. *World Journal of Orthopedics*, 6(1):8–16, 2015.

[20] Saebo. Range of motion exercises for spinal cord injuries. `https://www.saebo.com/range-motion-exercises-spinal-cord-injuries/`, 2017.

[21] H. Chester, R. J. Triolo, A. L. Elias, K. L. Kilgore, A. F. DiMarco, K. Bogie, A. H. Vette, M. Audu, R. Kobetic, S. R. Chang, K. Ming Chan, S. Dukelow, D. J. Bourbeau, S. W. Brose, K. J. Gustafson, Z. Kiss, and V. K. Mushahwar. Functional Electrical Stimulation and Spinal Cord Injury. *Physical Medicine and Rehabilitation Clinics of North America*, 25(3):631–ix, 2014.

[22] R. J. Downey, M. J. Bellman, H. Kawai, C. M. Gregory, and W. E. Dixon. Comparing the Induced Muscle Fatigue Between Asynchronous and Synchronous Electrical Stimulation in Able-Bodied and Spinal Cord Injured Populations. *IEEE Transactions on Neural Systems and Rehabilitation Engineering*, 23(6):964–972, 2015.

[23] Q. Zhang, M. Hayashibe, and D. Guiraud. Muscle Fatigue Tracking based on Stimulus Evoked EMG and Adaptive Torque Prediction. *2011 IEEE International Conference on Robotics and Automation*, 2011.

[24] M. O. Ibitoye, N. A. Hamzaid, N. Hasnan, A. K. A. Wahab, and G. M. Davis. Strategies for Rapid Muscle Fatigue Reduction during FES Exercise in Individuals with Spinal Cord Injury: A Systematic Review. *PLoS One*, 11(2):e0149024, 2016.

[25] J. M. Heasman, T. R. D. Scott, V. A. Vare, R. Y. Flynn, C. R. Gschwind, J. W. Middleton, and S. B. Rutkowski. Detection of Fatigue in the Isometric Electrical Activation of Paralyzed Hand Muscles of Persons with Tetraplegia. *IEEE Transactions on Rehabilitation Engineering*, 8(3):286–296, 2000.

[26] M. Yochum, S. Binczak, T. Bakir, S. Jacquir, and S. Lepers. A mixed fes/emg system for real time analysis of muscular fatigue. *2010 Annual International Conference of the IEEE Engineering in Medicine and Biology*, pages 4882–4885, 2010.

[27] R. K. Shields, S. Dudley-Javoroski, and K. R. Cole. Feedback-controlled stimulation enhances human paralyzed muscle performance. *Journal of Applied Physiology*, 101(5):1312–1319, 2006.

[28] N. K. Vøllestad. Measurement of human muscle fatigue. *Journal of Neuroscience Methods*, 74(2):219–227, 1997.

[29] N. Z. Mohamad, G. M. Hamzaid, N. Z.and Davis, A. K. Wahab, and N. Hasnan. Mechanomyography and Torque during FES-Evoked Muscle Contractions to Fatigue in Individuals with Spinal Cord Injury. *Sensors*, 17(7), 2017.

[30] R Merletti and P. A. Parker. *Electromyography: Physiology, Engineering, and Non-Invasive Applications*. John Wiley and sons, Inc., 2004.

[31] M. R. Al-Mulla, F. Sepulveda, and M. Colley. A Review of Non-Invasive Techniques to Detect and Predict Localised Muscle Fatigue. *Sensors*, 11(4):3545–3594, 2011.

[32] N.-Y. Yu, J.-J. Chen, and M.-S. Ju. Study of the Electrically Evoked EMG and Torque Output During the Muscle Fatigue Process in FES-Induced Static and Dynamic Contractions. *Basic and Applied Myology*, 9(1):11–18, 1999.

[33] N. A. Dimitrova, T. I. Arabadzhiev, J.-Y. Hogrel, and G.V. Dimitrov. Fatigue analysis of interference EMG signals obtained from biceps brachii during isometric voluntary contraction at various force levels. *Journal of Electromyography and Kinesiology*, 19(2):252–258, 2009.

[34] D. Tepavac and L. Schwirtlich. Detection and Prediction of FES-induced Fatigue. *Journal of Electromyography and Kinesiology*, 7(1):39–50, 1997.

[35] M. O. Ibitoye, Hamzaid N. A., J. M. Zuniga, N. Hasnan, and A. K. Wahab. Mechanomyographic Parameter Extraction Methods: An Appraisal for Clinical Applications. *Sensors*, 14(12):22940–22970, 2014.

[36] M. Shinohara and K. Søgaard. Mechanomyography for Studying Force Fluctuations and Muscle Fatigue. *Exerc Sport Sci Rev*, 34 2:59–64, 2006.

[37] M. A. Islam, K. Sundaraj, R. B. Ahmad, and N. U. Ahamed. Mechanomyogram for Muscle Function Assessment: A Review. *PLoS One*, 8(3), 2013.

[38] M. O. Ibitoye, N. A. Hamzaid, J. M. Zuniga, and A. K. Abdul Wahab. Mechanomyography and muscle function assessment: A review of current state and prospects. *Clinical Biomechanics*, 29(6):691–704, 2014.

[39] C. Orizio, B. Diemont, F. Esposito, E. Alfonsi, G. Parrinello, A. Moglia, and A. Veicsteinas. Surface mechanomyogram reflects the changes in the mechanical properties of muscle at fatigue. *European journal of applied physiology and occupational physiology*, 80(4):276–284, 1999.

[40] F. Khoshnoud and C. W. de Silva. Recent Advances in MEMS Sensor Technology - Biomedical Applications. *IEEE Instrumentation and Measurement Magazine*, 15(1):8–14, 2012.

[41] A. O. Posatskiy and T. Chau. The effects of motion artifact on mechanomyography: A comparative study of microphones and accelerometers. *Journal of*

Electromyography and Kinesiology, 22(2):320—-324, 2012.

[42] A. Jaskolska, P. Madeleine, A. Jaskolski, K. Kisiel-Sajewicz, and L. Arendt-Nielsen. A comparison between mechanomyographic condenser microphone and accelerometer measurements during submaximal isometric, concentric and eccentric contractions. *Journal of Electromyography and Kinesiology*, 17(3):336—-347, 2007.

[43] J. Lewis. Analog and digital mems microphone design considerations, 2013.

[44] Audio Precision. *Understanding PDM digital audio*, 2012.

[45] STMicroelectronics. *Getting started with the software package for STEVAL-STLKT01V1 based on STM32Cube*.

[46] J. Shi, Y.P. Zheng, X. Chen, and Q. H. Huang. Assessment of muscle fatigue using sonomyography: Muscle thickness change detected from ultrasound images. *Medical Engineering and Physics*, 29(4):472—479, 2007.

[47] J. Shi and Y.-P. Zheng. Continuous Monitoring of Sonomyography, Electromyography and Torque Generated by Normal Upper Arm Muscles During Isometric Contraction: Sonomyography Assessment for Arm Muscles. *IEEE Transactions On Biomedical Engineering*, 55(3):1191–1198, 2008.

[48] Y. Muramatsu and H. Kobayashi. Assessment of local muscle fatigue by NIRS - development and evaluation of muscle suit -. *ROBOMECH Journal*, 1(1):1–19, 2014.

[49] M. Watakabe, K. Mita, K. Akataki, and Y. Itoh. Mechanical behaviour of condenser microphone in mechanomyography. *Medical and Biological Engineering and Computing*, 39(2):195–201, 2001.

[50] STMicroelectronics. *Getting started with the STM32 ODE function pack for IoT node with BLE connectivity, digital microphone, environmental and motion sensors.*

[51] ST Microelectronics. *MP34DT04 - MEMS audio sensor omnidirectional digital microphone.*

[52] J. Lewis. *Understanding Microphone Sensitivity*, 2012.

[53] A. O. Posatskiy and T. Chau. Design and evaluation of a novel microphone-based mechanomyography sensor with cylindrical and conical acoustic chambers. *Medical Engineering and Physics*, 34(8):1184–1190, 2012.

[54] Knowles. *Product Data Sheet SPU1410LR5H-QB.*

[55] BITalino. *Electromyography (EMG) Sensor Data Sheet.*

[56] M. Cifrek, V. Medved, S. Tonkovic, and S. Ostojic. Surface EMG based muscle fatigue evaluation in biomechanics. *Clinical Biomechanics*, 24(4):327–340, 2009.

[57] R. Merletti and L. R. Lo Conte. Surface EMG Signal Processing During Isometric Contractions. *Journal of Electromyography and Kinesiology*, 7(4):241–250, 1997.

[58] F. Esposito, C. Orizio, and A. Veicsteinas. Electromyogram and mechanomyogram changes in fresh and fatigued muscle during sustained contraction in men. *European Journal of Applied Physiology and Occupational Physiology*, 78(6):494–501, 1998.

[59] J. P. Weir, K. M. Ayers, J. F. Lacefield, and K. L. Walsh. Mechanomyographic and electromyographic responses during fatigue in humans: influence of muscle length. *European Journal of Applied Physiology*, 81(4):352–359, 2000.

[60] M. Tarata. Mechanomyography versus Electromyography, in monitoring the muscular fatigue. *BioMedical Engineering OnLine*, 2(1), 2003.

[61] A. Rainoldi, J. E. Bullock-Saxton, F. Cavarretta, and N. Hogan. Repeatability of maximal voluntary force and of surface EMG variables during voluntary isometric contraction of quadriceps muscles in healthy subjects. *Journal of Electromyography and Kinesiology*, 11(6):425–438, 2001.

[62] P. ad Ge H.-y. Madeleine, A. Jaskolska, D. Farina, A. Jaskolski, and L. Arendt-Nielsen. Spectral moments of mechanomyographic signals recorded with accelerometer and microphone during sustained fatiguing contractions. *Medical and Biological Engineering and Computing*, 44(4):290–297, 2006.

[63] F. Rossi, P. Motto Ros, and D. Demarchi. Live Demonstration: Low Power System for Event-Driven Control of Functional Electrical Stimulation. *2018 IEEE International Symposium on Circuits and Systems (ISCAS)*, pages 1–1, 2018.

[64] P. Sampson, C. Freeman, S. Coote, S. Demain, P. Feys, K. Meadmore, and A-M. Hughes. Using Functional Electrical Stimulation Mediated by Iterative Learning Control and Robotics to Improve Arm Movement for People With Multiple Sclerosis. *IEEE Transactions On Neural Systems And Rehabilitation Engineering*, 24(2):1–1, 2016.

[65] P.L. Melo, M.T. Silva, J.M. Martins, and D.J. Newman. Technical developments of functional electrical stimulation to correct drop foot: Sensing, actuation and control strategies. *Cinical Biomechanics*, 30:101–113, 2015.

[66] T. Paillard. Combined Application of Neuromuscular Electrical Stimulation and Voluntary Muscular Contractions. *Sports Medicine*, 38(2):161–177, 2008.

[67] J. Taradaj, T. Halski, M. Kucharzewski, K. Walewicz, A. Smykla, M. Ozon, L. Slupska, R. Dymarek, K. Ptaszkowski, J. Rajfur, and M. Pasternok. The Effect of NeuroMuscular Electrical Stimulation on Quadriceps Strength and Knee Function in Professional Soccer Players: Return to Sport after ACL Reconstruction. *BioMed Research International*, 2013:802534, 2013.

Personal Thanks

Sono incredibilmente orgogliosa del mio percorso universitario e di questo lavoro, principalmente perché sono stati entrambi realizzati grazie al supporto e l'aiuto delle persone meravigliose che compongono la mia famiglia e i miei amici. Un grazie infinito a tutti voi, le parole non saranno mai abbastanza per esprimere il mio affetto.

Ai miei genitori, grazie per l'infinita fiducia, il costante supporto e per avermi regalato quelle parti del mio carattere che mi permettono di portarvi sempre con me.

A mia sorella Gaia, grazie per essere così simile a me e così diversa, e per ricordarmi sempre che non potrò mai essere sola.

A mia nonna Raffaella, per avermi sempre ascoltata e sostenuta durante tutto il percorso.

To Riccardo, thanks for *always* being my lobster, my lighthouse and my pink bow in the pocket.

A Faby, grazie per aver condiviso con me ogni momento importante, per le nostre chiacchierate di cui avró sempre bisogno e per aver sempre occupato il solo e unico ruolo di Best.

A Lucrezia, grazie perchè mi hai illustrato concetti impossibili con le metafore più geniali, per aver cantato a squarciagola Misery Business con me e per la nostra amicizia unica.

Alla mia famiglia fuorisede, Giulia, Federica e Vito, grazie per aver condiviso con me questi anni, per avermi fatto scoprire mille tipi di cibo diversi, per avermi regalato tutti gli indimenticabili momenti insieme. Non bastiamo per un calcetto, ma siamo una squadra stupenda.

A Silvia, grazie per le avventure che solo la convivenza puó riservare, e per essere sempre riuscita a farmi ridere durante ognuna di esse, facendomi sentire a casa.

A Sebo, grazie per tutti i momenti condivisi a parlare di Pokèmon, draghetti e a volte anche di università, rendendo tutto più bello.

A Giorgio, Atena, Anna, Isabella e Ilaria, grazie per dimostrarmi da sempre che l'amicizia va oltre il tempo e la distanza.

A Marta, Martina, Alessandra e Chiara, grazie per aver sconfitto il troll insieme e per l'inevitabile legame di amicizia che ne consegue.

A Robi, Alberto, Maurizio, Fabio, Sofy2 e a tutto il gruppo del Civera, grazie per i brainstorming, le lezioni di saldatura e le briscole, tutti fondamentali per lo svolgimento di questa tesi.

To Lucia, Eleonora, Giovanni, Fra S., Fra C., Giulia, Ivan, Fon and to all the LSI people, thank you for your friendship, the snowball fights and the Harry Potter trivials.

To J.K. Rowling, for creating a world where I will *always* be able to wonder while finding myself.

"Tutto il resto era ancora nulla.
Inventarlo - questo sarebbe stato
meraviglioso."

[A. Baricco, Oceano Mare]